EFFICIENT FINITE ELEMENT METHODS FOR SEMICLASSICAL NONLINEAR SCHRÖDINGER EQUATIONS WITH RANDOM POTENTIALS*

PANCHI LI† AND ZHIWEN ZHANG†

Abstract. In this paper, we propose two time-splitting finite element methods to solve the semiclassical nonlinear Schrödinger equation (NLSE) with random potentials. We then introduce the multiscale finite element method (MsFEM) to reduce the degrees of freedom in physical space. In the MsFEM approach, we construct multiscale basis functions by solving optimization problems and study two time-splitting MsFEMs for the semiclassical NLSE with random potentials. We provide convergence analysis for the proposed methods and show that they achieve second-order accuracy in both spatial and temporal spaces and an almost first-order convergence rate in the random space. In addition, we present a multiscale reduced basis method to reduce the computational cost of constructing basis functions for solving random NLSEs. Finally, we present several 1D and 2D numerical examples to confirm the convergence of our methods and investigate wave propagation in the NLSE with random potentials.

Key words. Semiclassical nonlinear Schrödinger equation; finite element method; multiscale finite element method; random potential; time-splitting methods.

MSC codes. 35Q55, 65M60, 81Q05, 47H40

1. Introduction.

The nonlinear Schrödinger equation (NLSE) is a prototypical dispersive nonlinear equation that has been extensively used to study the Bose-Einstein condensation, laser beam propagation in nonlinear optics, particle physics, semi-conductors, superfluids, etc. In the presence of random potentials, the interaction of nonlinearity and random effect poses challenges to understanding intriguing phenomena, such as localization and delocalization [20, 25, 40, 48] and the soliton propagation [24, 33, 45]. Owing to the inherent challenges in obtaining analytical solutions and the limited experimental observations in nonlinear random media, numerical simulations play a crucial role in understanding and investigating the nonlinear dynamics in such regimes, particularly for long-time behaviors in high-dimensional physical space. This necessitates high-resolution and efficient numerical methods for the NLSE with random potentials.

In the past decades, numerous numerical methods have been proposed for the NLSE with deterministic potentials, and recent comparisons can be found in [4, 6, 29]. For the time-dependent NLSE, the implicit Crank-Nicolson (CN) schemes were extensively employed to conserve the mass and energy of the system. The CN method is known for its lower efficiency in handling nonlinearity since iteration methods and time step conditions are required [2, 38, 46]. To enhance computational efficiency, several promising approaches have been proposed, including linearized implicit methods [51, 55], relaxation methods [10, 12] and time-splitting methods [9, 11, 50]. Among these, time-splitting methods exhibit outstanding performance in terms of efficiency since linear equations with constant coefficients are solved at each time step. To reach optimal accuracy, time-splitting type schemes ask for enough smoothness on both the

*Submitted to the editors DATE.

Funding: The research of Z. Zhang is supported by the National Natural Science Foundation of China (project 12171406), the Hong Kong RGC grant (projects 17300318 and 17307921), the Outstanding Young Researcher Award of HKU (2020–21), Seed Funding for Strategic Interdisciplinary Research Scheme 2021/22 (HKU), and seed funding from the HKU-TCL Joint Research Center for Artificial Intelligence.

†Department of Mathematics, The University of Hong Kong (lipch@hku.hk, zhangzw@hku.hk).

potential and the initial condition. Such as Strang splitting methods demand the initial condition to possess H^4 regularity [11]. The low-regularity time-integrator methods [35, 41, 54] are proposed to alleviate such constraint. Nevertheless, the low-regularity time-integrator methods rely on the Fourier discretization in space with a periodical setup, and their integration with finite difference methods (FDM) and finite element methods (FEM) has not been established. The spatial Fourier discretization allows the spectral methods to have exponential convergence for smooth potentials and competitive efficiency in simulations. With the random potential further considered, the spectral discretization with the Monte Carlo (MC) sampling [54] and quasi-Monte Carlo (qMC) sampling [53] have been employed for the 1D case. Nonetheless, spectral methods may not maintain their optimal convergence rate in cases of non-smooth potentials. This motivates us to develop numerical methods to efficiently solve NLSEs with random potentials within the framework of FEM in this work.

To develop efficient FEM methods to solve PDEs, intense research efforts in dimensionality reduction methods by constructing the multiscale reduced basis functions have been invested (see, e.g., [1, 3, 16, 21, 22, 23, 28, 31, 43]). Incorporating the local microstructures of the differential operator into the basis functions, the multiscale FEM (MsFEM) can capture the large-scale components of the multiscale solution on a coarse mesh without the need to resolve all the small-scale features on a fine mesh. Recently, the localized orthogonal decomposition method [3] has been proposed to solve the stationary and time-dependent NLSE with deterministic potentials [19, 27], which could produce eigenvalues and solution with high order accuracy.

Motivated by the MsFEM for elliptic problems with random coefficients [30, 32] and the linear Schrödinger equation with multiscale and random potentials [15], we generate the multiscale basis functions by solving a set of equality-constrained quadratic programs. We find that the localized orthogonal normalization constraints of optimal problems imply a mesh-dependent scale in the basis functions. This scale in the linear algebraic equation is eliminated naturally. However, when the cubic nonlinearity is coupled, the balance of such scale in the equation is broken, which produces an indispensable scale in the numerical solution. In this work, we add a mesh-dependent factor to the orthogonality constraints to eliminate this scale of basis functions. We use these new basis functions to discrete the deterministic NLSE that reduces the degrees of freedom (dofs) for FEM without accuracy lost.

For the time-marching, we present two Strang splitting methods. One of the methods solves the linear Schrödinger equation using the eigendecomposition method [15] and the cubic ordinary differential equation at each time step, and it can maintain the convergence rate even for the discontinuous potential. Meanwhile, we parameterize the random potential with the Karhunen-Loève (KL) expansion method. Instead of the traditional MC sampling method, we employ the qMC method to generate random samples. It is shown that the proposed approaches yield the second-order accurate solution in both time and space and almost the first-order convergence rate with respect to the sampling number. Theoretically, we give the convergence analysis of the L^2 error estimate of the time-splitting FEM (TS-FEM) for the deterministic NLES, which is further extended for the estimate of the time-splitting MsFEM (TS-MsFEM) for the NLSE with random potentials. We verify several theoretical aspects in numerical experiments. Besides, we propose a multiscale reduced basis method to decrease the construction of multiscale basis functions for random potentials, which can further improve the simulation efficiency. By the proposed numerical methods, we investigate the wave propagation for the NLSE with parameterized random potentials in both 1D and 2D physical space. We observe the localized phenomena of mass density of the linear case, while the significant delocalization of the NLSE with strong nonlinearity.

The rest of the paper is organized as follows. In section 2, we describe fundamental model problems. The FEM and MsFEM with time-splitting methods for the deterministic NLSE are presented in section 3. Analysis results are presented in section 4. Numerical experiments, including 1D and 2D examples, are conducted in section 5. Conclusions are drawn in section 6.

2. The semiclassical NLSE with random potentials. The fundamental model considered in this manuscript is

$$\begin{cases} i\epsilon\partial_t\psi^\epsilon = -\frac{\epsilon^2}{2}\Delta\psi^\epsilon + v(\boldsymbol{x},\omega)\psi^\epsilon + \lambda|\psi^\epsilon|^2\psi^\epsilon, \quad \boldsymbol{x}\in\mathcal{D}, \quad \omega\in\Omega, \quad t\in(0,T], \\ \psi^\epsilon|_{t=0} = \psi_{\text{in}}(\boldsymbol{x}), \end{cases} \tag{2.1}$$

where $0 < \epsilon \ll 1$ is an effective Planck constant, $\mathcal{D} \subset \mathbb{R}^d (d = 1, 2, 3)$ is a bounded domain, $\omega \in \Omega$ is the random sample with Ω being the random space, T is the terminal time, $\psi_{\text{in}}(\boldsymbol{x})$ denotes the initial state, $v(\mathbf{x}, \boldsymbol{\omega})$ is a given random potential, and $\lambda\ (\geq 0)$ is the nonlinearity coefficient. The periodic boundary is considered in this work. Physically, $|\psi^\epsilon|^2$ denotes the mass density and the system's total mass $m_T = \int_{\mathcal{D}} |\psi_{\text{in}}|^2 \mathrm{d}\boldsymbol{x}$ is conserved by (2.1). Note that the wave function $\psi^\epsilon : [0,T]\times\mathcal{D}\times\Omega \to \mathbb{C}$, and the function space $H_P^1(\mathcal{D}) = H_P^1(\mathcal{D}, \mathbb{C})$, in which the functions are periodic over domain $\mathcal{D}$. The inner product is defined as $(v, w) = \int_{\mathcal{D}} v\overline{w}\mathrm{d}\boldsymbol{x}$ with $\overline{w}$ denoting the complex-conjugate of w, and the L^2 norm is $\|w\|^2 = \||w|\|^2 = (w, w)$.

The Hamiltonian operator $\mathcal{H}$ of the nonlinear system has the form

$$\mathcal{H}(\cdot) = -\frac{\epsilon^2}{2}\Delta(\cdot) + v(\cdot) + \lambda|\cdot|^2(\cdot). \tag{2.2}$$

Owing to the Hamiltonian operator is not explicitly dependent on time, and the commutator $[\mathcal{H}, \mathcal{H}] = 0$, the energy of the system,

$$E(t) = (\mathcal{H}\psi^\epsilon, \psi^\epsilon) = \frac{\epsilon^2}{2}\|\nabla\psi^\epsilon\|^2 + (v(\mathbf{x}, \boldsymbol{\omega}), |\psi^\epsilon|^2) + \frac{\lambda}{2}\|\psi^\epsilon\|_{L^4}^4, \tag{2.3}$$

remains unchanged as time evolves,i.e., $\mathrm{d}_t E(t) = 0$ for all $t > 0$.

ASSUMPTION 2.1. *We assume the potential $v(\boldsymbol{x}, \omega)$ is bounded in $L^\infty(\Omega; H^s)$ with $0 \leq s \leq 2$. More precisely, the bound of $\|v(\boldsymbol{x}, \omega)\|_\infty$ satisfies*

$$\|v(\boldsymbol{x}, \omega)\|_\infty \lesssim \frac{\epsilon^2}{H^2}, \tag{2.4}$$

where $\lesssim$ means bounded by a constant, and H is the size of coarse mesh.

We first consider the deterministic potential, i.e., $v(\boldsymbol{x}, \omega) = v(\boldsymbol{x})$. Assume that there exists a finite time T such that $\psi^\epsilon \in L^\infty([0,T]; H^4) \cap L^1([0,T]; H^2)$ and by Sobolev embedding theorem, we have $\|\psi^\epsilon\|_\infty \leq C\|\psi^\epsilon\|_{H^2}$ for $d \leq 3$. In the sequel, we will use a uniform constant C to denote all the controllable constants that are independent of ϵ for simplicity of notation.

LEMMA 2.1. *Let ψ^ϵ be the solution of (2.1), and assume $\psi^\epsilon \in L^\infty([0,T]; H^4) \cap L^1([0,T]; H^2)$. If $\partial_t\psi^\epsilon(t) \in H^s$ with $s = 0, 1, 2$ for all $t \in [0,T]$, there exists a constant $C_{\lambda,\epsilon}$ such that*

$$\|\partial_t\psi^\epsilon\|_{H^s} \leq C_{\lambda,\epsilon}, \tag{2.5}$$

where $C_{\lambda,\epsilon}$ mainly depends on ϵ and λ. In particular, for $d=3$ and $s=1,2$, we have a compact formulate

$$\|\partial_t \nabla^s \psi^\epsilon\| \leq \left(\frac{\|\nabla v\|_\infty + C\lambda \|\nabla^{s+1}\psi^\epsilon\|}{\epsilon}\right) \|\partial_t \nabla^{s-1}\psi^\epsilon\| \exp\left(\frac{C\lambda T(\|\nabla^2 \psi^\epsilon\| + \|\psi^\epsilon\|_\infty^2)}{\epsilon}\right),$$

where

$$\|\partial_t \psi^\epsilon\| \leq \frac{C}{\epsilon} \exp\left(\frac{2\lambda T \|\psi^\epsilon\|_\infty^2}{\epsilon}\right). \tag{2.6}$$

The proof is detailed in Appendix B. Note that for $\lambda = 0$, the result of this lemma degenerates to the estimate of the linear Schrödinger equation as in [8, 52].

Next, we assume that $v(\boldsymbol{x}, \omega)$ is a second-order random field with a mean value $\mathbb{E}[v(\boldsymbol{x}, \omega)] = v(\boldsymbol{x})$ and a covariance kernel denoted by $C(\boldsymbol{x}, \boldsymbol{y})$. In this study, we adopt the covariance kernel

$$C(\boldsymbol{x}, \boldsymbol{y}) = \sigma^2 \exp\left(-\sum_{i=1}^{d} \frac{|x_i - y_j|^2}{2l_i^2}\right), \tag{2.7}$$

where σ is a constant and l_i denotes the correlation lengths in each dimension. Moreover, we also assume that the random potential is almost surely bounded. Using the KL expansion method [34, 37], the random potential takes the form

$$v(\boldsymbol{x}, \boldsymbol{\omega}) = \bar{v}(\boldsymbol{x}) + \sum_{j=1}^{\infty} \sqrt{\lambda_j} \xi_j(\omega) v_j(\boldsymbol{x}), \tag{2.8}$$

where $\xi_i(\omega)$ represents mean-zero and uncorrelated random variables, and $\{\lambda_i, v_i(\boldsymbol{x})\}$ are the eigenpairs of the covariance kernel $C(\boldsymbol{x}, \boldsymbol{y})$. The eigenvalues are sorted in descending order and the decay rate depends on the regularity of the covariance kernel [47]. Hence the random potential can be parameterized by the truncated form

$$v_m(\boldsymbol{x}, \boldsymbol{\omega}) = \bar{v}(\boldsymbol{x}) + \sum_{j=1}^{m} \sqrt{\lambda_j} \xi_j(\omega) v_j(\boldsymbol{x}). \tag{2.9}$$

Once the random potential is parameterized, the wave function ψ_m^ϵ obeys

$$\begin{cases} i\epsilon \partial_t \psi_m^\epsilon = -\dfrac{\epsilon^2}{2} \Delta \psi_m^\epsilon + v_m(\boldsymbol{x}, \boldsymbol{\omega}) \psi_m^\epsilon + \lambda |\psi_m^\epsilon|^2 \psi_m^\epsilon, & \boldsymbol{x} \in \mathcal{D}, \omega \in \Omega, t \in (0, T], \\ \psi_m^\epsilon(t=0) = \psi_{\text{in}}. \end{cases} \tag{2.10}$$

The residual of $|v_m(\boldsymbol{x}, \boldsymbol{\omega}) - v(\boldsymbol{x}, \boldsymbol{\omega})|$ relies on the regularity of eigenfunctions and the decay rate of eigenvalues. We make the following assumption for the parameterized random potentials.

Assumption 2.2.
1. *In the KL expansion* (2.9)*, assume that there exist constants $C > 0$ and $\Theta > 1$ such that $\lambda_j \leq C j^{-\Theta}$ for all $j \geq 1$.*
2. *The eigenfunctions $v_j(\boldsymbol{x})$ are continuous and there exist constants $C > 0$ and $0 \leq \eta \leq \frac{\Theta - 1}{2\Theta}$ such that $\|v_j\|_{H^2} \leq C\lambda_j^{-\eta}$ for all $j \geq 1$.*

3. *Assume that the parameterized potential* v_m *satisfies*

$$\|v - v_m\|_\infty \le C m^{-\chi}, \quad \sum_{j=1}^{\infty} (\sqrt{\lambda_j} \|v_j\|_{H^2})^p < \infty,$$

for some positive constants C *and* χ, *and* $p \in (0, 1]$.

In [53], the authors provide the $L^\infty([0,T], H^1)$ error between wave functions to (2.1) and (2.10) for the 1D case. Here we get a similar result for the L^2 error between the wave functions for $d \le 3$.

LEMMA 2.2. *The error between wave functions to* (2.1) *and* (2.10) *satisfies*

$$\|\psi_m^\epsilon - \psi^\epsilon\| \le \frac{2\|v_m - v\|_\infty}{\epsilon} \exp\left(\frac{2T\lambda}{\epsilon} \|\psi^\epsilon\|_\infty \|\psi_m^\epsilon\|_\infty\right). \tag{2.11}$$

Proof. Define $\delta\psi = \psi_m^\epsilon - \psi^\epsilon$ and it satisfies

$$i\epsilon \partial_t \delta\psi = -\frac{\epsilon^2}{2} \Delta \delta\psi + v_m \delta\psi + (v_m - v)\psi^\epsilon + \lambda(|\psi_m^\epsilon|^2 \psi_m^\epsilon - |\psi^\epsilon|^2 \psi^\epsilon) \tag{2.12}$$

with the initial condition $\delta\psi(t = 0) = 0$. For the nonlinear term, we have

$$|\psi_m^\epsilon|^2 \psi_m^\epsilon - |\psi^\epsilon|^2 \psi^\epsilon = |\psi_m^\epsilon|^2 \delta\psi + \psi^\epsilon \psi_m^\epsilon \delta\bar{\psi} + |\psi^\epsilon|^2 \delta\psi.$$

Taking the inner product of (2.12) with $\delta\psi$ yields

$$i\epsilon \mathrm{d}_t \|\delta\psi\|^2 = \big((v_m - v)\psi^\epsilon, \delta\psi\big) - \big((v_m - v)\bar{\psi}^\epsilon, \delta\bar{\psi}\big) + \lambda\big((\psi^\epsilon \delta\bar{\psi}, \bar{\psi}_m^\epsilon \delta\psi) - (\bar{\psi}^\epsilon \delta\psi, \psi_m^\epsilon \delta\bar{\psi})\big).$$

We further get

$$\begin{aligned} \mathrm{d}_t \|\delta\psi\|^2 &\le \frac{2\|v_m - v\|_\infty}{\epsilon} \int_{\mathcal{D}} |\psi^\epsilon||\delta\psi| \mathrm{d}\boldsymbol{x} + \frac{2\lambda}{\epsilon} \int_{\mathcal{D}} |\psi^\epsilon \delta\psi||\psi_m^\epsilon \delta\psi| \mathrm{d}\boldsymbol{x} \\ &\le \frac{2\|v_m - v\|_\infty}{\epsilon} \|\psi^\epsilon\|\|\delta\psi\| + \frac{2\lambda}{\epsilon} \|\psi^\epsilon\|_\infty \|\psi_m^\epsilon\|_\infty \|\delta\psi\|^2. \end{aligned}$$

Owing to the $L^\infty([0,T] \times \Omega; H^s)$ bound of both ψ^ϵ and ψ_m^ϵ, an application of Gronwall inequality yields ∎

$$\|\delta\psi\| \le \frac{2T\|v_m - v\|_\infty}{\epsilon} \exp\left(\frac{2T\lambda}{\epsilon} \|\psi^\epsilon\|_\infty \|\psi_m^\epsilon\|_\infty\right).$$

Owing to the assumption $\|v_m - v\|_\infty \le C m^{-\chi}$, this lemma implies that $\psi_m^\epsilon \to \psi^\epsilon$ as $m \to \infty$.

3. Numerical methods. Consider the regular mesh $\mathcal{T}_h$ of $\mathcal{D}$. The standard P_1 finite element space on the mesh $\mathcal{T}_h$ is given by $P_1(\mathcal{T}_h) = \{v \in L^2(\bar{\mathcal{D}}) |$ for all $K \in \mathcal{T}_h, v|_K$ is a polynomial of total degree $\le 1\}$. Then the $H_P^1(\mathcal{D})$-confirming finite element spaces are $V_h = P_1(\mathcal{T}_h) \cap H_P^1(\mathcal{D})$ and $V_H = P_1(\mathcal{T}_H) \cap H_P^1(\mathcal{D})$. Denote $V_h = span\{\phi_1^h, \cdots, \phi_{N_h}^h\}$ and $V_H = span\{\phi_1^H, \cdots, \phi_{N_H}^H\}$, where N_h and N_H are the corresponding number of vertices. The wave function is approximated by $\psi_h^\epsilon(t, \boldsymbol{x}) = \sum_p^{N_h} U_p(t) \phi_p^h(\boldsymbol{x})$ on the fine mesh, where $U_p(t) \in \mathbb{C}, p = 1, \cdots, N_h$ and $t \in [0, T]$.

3.1. TS-FEM for the NLSE. In the case of nontrivial potentials, the numerical mass density may decay towards zero with an exponential rate when utilizing the direct Backward Euler method. Time-splitting manners can maintain the mass of the system. Therefore, we adopt Strang splitting methods for time-stepping. The NLSE is rewritten to

$$i\epsilon\partial_t\psi^\epsilon = (\mathcal{L}_1 + \mathcal{L}_2)\psi^\epsilon, \tag{3.1}$$

and its exact solution has the form $\psi^\epsilon(t) = S^t\psi_{\text{in}}$, where $S^t = \exp(-i(\mathcal{L}_1 + \mathcal{L}_2)t/\epsilon)$. To efficiently handle the nonlinear term, we present two alternative approaches, both of which require solving linear equations:

1. Option 1,

$$\mathcal{L}_1(\cdot) = -\frac{\epsilon^2}{2}\Delta(\cdot) + v(\cdot), \quad \mathcal{L}_2(\cdot) = \lambda|\cdot|^2(\cdot). \tag{3.2}$$

2. Option 2,

$$\mathcal{L}_1(\cdot) = -\frac{\epsilon^2}{2}\Delta(\cdot), \quad \mathcal{L}_2(\cdot) = v(\cdot) + \lambda|\cdot|^2(\cdot). \tag{3.3}$$

When computing the commutator $[\mathcal{L}_1, \mathcal{L}_2] = \mathcal{L}_1\mathcal{L}_2 - \mathcal{L}_2\mathcal{L}_1$, the regularity of potential $v \in C^2(\mathcal{D})$ is required for Option 2, whereas Option 1 does not need this requirement.

From t_n to t_{n+1}, the Strang splitting yields

$$\psi^{\epsilon,n+1} := \mathcal{L}\psi^{\epsilon,n} = \exp\left(-\frac{i\Delta t}{2\epsilon}\mathcal{L}_2(\cdot)\right) \circ \exp\left(-\frac{i\Delta t}{\epsilon}\mathcal{L}_1\right) \exp\left(-\frac{i\Delta t}{2\epsilon}\mathcal{L}_2(\cdot)\right) \circ \psi^{\epsilon,n}. \tag{3.4}$$

This formulation can be written as

$$\psi^{\epsilon,n+1} = \exp\left(-\frac{i\Delta t}{\epsilon}(\mathcal{L}_1 + \mathcal{L}_2(\psi^{\epsilon,n}))\right)\psi^{\epsilon,n} + \mathcal{R}_1^n. \tag{3.5}$$

By the Taylor expansion, we have $\|\mathcal{R}_1^n\| = \mathcal{O}\left(\frac{\Delta t^3}{\epsilon^3}\right)$. Furthermore, we define the n-fold composition

$$\psi^{\epsilon,n} = \mathcal{L}^n\psi_{\text{in}} = \underbrace{\mathcal{L}(\Delta t, \cdot) \circ \cdots \circ \mathcal{L}(\Delta t, \cdot)}_{n \text{ times}}\psi_{\text{in}} \tag{3.6}$$

Next, we introduce the classical finite element discretization for the operator $\mathcal{L}_1$. Define the weak form

$$i\epsilon(\partial_t\psi^\epsilon, \phi) = a(\psi^\epsilon, \phi), \quad \forall\phi \in H_P^1(\mathcal{D}), \tag{3.7}$$

where $a(\psi^\epsilon, \phi)$ is determined by the option of $\mathcal{L}_1$. For example, setting $\mathcal{L}_1 = -\frac{\epsilon^2}{2}\Delta + v$, we have $a(\psi^\epsilon, \phi) = \frac{\epsilon^2}{2}(\nabla\psi^\epsilon, \nabla\phi) + (v\psi^\epsilon, \phi)$ and the Galerkin equations

$$i\epsilon\sum_p \mathrm{d}_t U_p(\phi_p^h, \phi_q^h) = \frac{\epsilon^2}{2}\sum_p U_p(t)(\phi_p^h, \phi_q^h) + \sum_p U_p(t)(v\phi_p^h, \phi_q^h) \tag{3.8}$$

with $q = 1, \cdots, N_h$. The corresponding matrix form is

$$i\epsilon M^h \mathrm{d}_t U(t) = \left(\frac{\epsilon^2}{2}S^h + V^h\right)U(t), \tag{3.9}$$

where $U(t)$ is a vector with $U(t) = (U_1(t), \cdots, U_{N_h}(t))^T$, $M^h = [M^h_{pq}]$ is the mass matrix with $M^h_{pq} = (\phi^h_p, \phi^h_q)$, $S^h = [S^h_{pq}]$ is the stiff matrix with $S^h_{pq} = (\nabla\phi^h_p, \nabla\phi^h_q)$, and $V^h = [V^h_{pq}]$ is the potential matrix with $V^h_{pq} = (v\phi^h_p, \phi^h_q)$.

We now present the formal TS-FEM methods for the deterministic NSLE. The first one is the discretized counterpart of Option 1:

$$\begin{aligned} \tilde{U}^n &= \exp\left(-\frac{i\lambda\Delta t}{2\epsilon}|U^n|^2\right)U^n, \\ \tilde{U}^{n+1} &= P\exp\left(-\frac{i\Delta t}{\epsilon}\Lambda\right)(P^{-1}\tilde{U}^n), \\ U^{n+1} &= \exp\left(-\frac{i\lambda\Delta t}{2\epsilon}|\tilde{U}^{n+1}|^2\right)\tilde{U}^{n+1}, \end{aligned} \tag{3.10}$$

where $(M^h)^{-1}(\frac{\epsilon^2}{2}S^h + V^h) = P\Lambda P^{-1}$ with Λ being a diagonal matrix. We call it **SI** in the remaining of this paper. Owing to the application of the eigendecomposition method [15], the error in time is mainly contributed by the time-splitting manner. Meanwhile, this scheme does not require time step size $\Delta t = o(\epsilon)$, although the full linear semiclassical Schrödinger equation must be solved.

Option 2 has been extensively used in previous works, such as [7, 9]. In the FEM framework, it solves the NLES in the following procedures:

$$\begin{aligned} \tilde{U}^n &= \exp\left(-\frac{i\Delta t}{2\epsilon}(v + \lambda|U^n|^2)\right)U^n, \\ iM^h\left(\frac{\tilde{U}^{n+1} - \tilde{U}^n}{\Delta t}\right) &= \frac{\epsilon}{2}S^h\left(\frac{\tilde{U}^{n+1} + \tilde{U}^n}{2}\right), \\ U^{n+1} &= \exp\left(-\frac{i\Delta t}{2\epsilon}(v + \lambda|\tilde{U}^{n+1}|^2)\right)\tilde{U}^{n+1}. \end{aligned} \tag{3.11}$$

This method requires the mesh size $h = \mathcal{O}(\epsilon)$ and time step size $\Delta t = \mathcal{O}(\epsilon)$ [9], and we call it **SII** in the remaining of this paper.

Denote L the discretized counterpart of $\mathcal{L}$, and similarly, L_1 and L_2 their respective discretized versions. From t_n to t_{n+1}, the discretized solution in both time and space can be determined by the recurrence

$$U^{n+1} = L(\Delta t, U^n)U^n = L_2\left(\frac{\Delta t}{2}, L_1(\Delta t)L_2\left(\frac{\Delta t}{2}, U^n\right)\right)U^n. \tag{3.12}$$

Denote $\psi^{\epsilon,n}_h = \sum_{p=1}^{N_h} U^n_p\phi^h_p$, and for simplicity we employ a formal notation for the n-fold composition

$$\psi^{\epsilon,n}_h = L^n\psi^0_h = \underbrace{L(\Delta t,\cdot)\circ\cdots\circ L(\Delta t,\cdot)}_{n\text{ times}}\psi^0_h, \tag{3.13}$$

where $\psi^0_h = R_h\psi_{\text{in}}$ with R_h being the Ritz projection operator.

3.2. MsFEM for the deterministic NLSE. Instead of the FEM, we construct the multiscale basis functions to reduce dofs in computations. The P_1 FEM basis functions on both the coarse mesh $\mathcal{T}_H$ and fine mesh $\mathcal{T}_h$ are required. To describe the localized property of multiscale basis functions, here we define a series of nodal patches $\{D_\ell\}$ associated with $\boldsymbol{x}_p \in \mathcal{N}_H$ as

$$D_0(\boldsymbol{x}_p) := \text{supp}\{\phi_p\} = \cup\{K \in \mathcal{T}_H \mid \boldsymbol{x}_p \in K\},$$
$$D_\ell := \cup\{K \in \mathcal{T}_H \mid K \cap \overline{D_{\ell-1}} \neq \emptyset\}, \quad \ell = 1, 2, \cdots .$$

The multiscale basis functions are obtained by solving the optimization problems

$$\phi_p = \arg \min_{\phi \in H_P^1(\mathcal{D})} a(\phi, \phi), \tag{3.14}$$

$$\text{s.t.} \int_{\mathcal{D}} \phi \phi_q^H \mathrm{d}\mathbf{x} = \lambda(H) \delta_{pq}, \quad \forall 1 \leq q \leq N_H, \tag{3.15}$$

where $a(\phi, \phi) = \frac{\epsilon^2}{2}(\nabla\phi, \nabla\phi) + (v\phi, \phi)$, and $\lambda(H) = 1$ in the previous work [13, 14, 15, 30, 36]. Note that the localized constraint is not considered in the optimal problems, thus we obtain the global basis functions.

In this work, we set $\lambda(H) = (1, \phi_q^H)$, and it can be computed explicitly. Since P_1 basis functions are used, we have $\lambda(H) = H$ for 1D. To explain this setup, we introduce the weighted Clément-type quasi-interpolation operator [28]

$$I_H : H_P^1(\mathcal{D}) \to V_H, \quad f \mapsto I_H(f) := \sum_p \frac{(f, \phi_p^H)}{(1, \phi_p^H)} \phi_p^H. \tag{3.16}$$

The high-resolution finite element space $V_h = V_H \oplus W_h$, where W_h is the kernel space of I_H. And for all $f \in H_P^1 \cap H^2$, it holds [39]

$$\|f - I_H(f)\| \leq H^2 \|f\|_{H^2}. \tag{3.17}$$

In the MsFEM space, the wave function ψ^ϵ is approximated with

$$\psi^\epsilon(\boldsymbol{x}) \approx \sum_{p=1}^{N_H} \hat{U}_p \phi_p. \tag{3.18}$$

It can be projected onto the coarse mesh by I_H,

$$I_H(\psi^\epsilon) = \sum_{p=1}^{N_H} \frac{(\sum_{q=1}^{N_H} \hat{U}_q \phi_q, \phi_p^H)}{(1, \phi_p^H)} \phi_p^H = \sum_{p=1}^{N_H} \frac{\lambda(H)\hat{U}_p}{(1, \phi_p^H)} \phi_p^H.$$

If ψ^ϵ is continuous at $\boldsymbol{x}_p$, the above formula indicates that at node $\boldsymbol{x}_p$,

$$\psi^\epsilon(\boldsymbol{x}_p) \approx \frac{\lambda(H)\hat{U}_p}{(1, \phi_p^H)}.$$

Let $\lambda(H) = 1$, we can see that it holds $\psi^\epsilon(\boldsymbol{x}_p) \approx \hat{U}_p/(1, \phi_p^H)$ in the MsFEM space. Take an assumption that $\hat{\phi}_p = (1, \phi_p^H)\phi_p$, where $\hat{\phi}_p$ is independent of the mesh size H. Then, (3.18) can be rewritten to

$$\psi^\epsilon(\boldsymbol{x}) \approx \sum_{p=1}^{N_H} \psi^\epsilon(\boldsymbol{x}_p)(1, \phi_p^H)\phi_p = \sum_{p=1}^{N_H} \psi^\epsilon(\boldsymbol{x}_p)\hat{\phi}_p. \tag{3.19}$$

Note that $\hat{\phi}_p$ is still the multiscale basis function at $\boldsymbol{x}_p$. We consider the following two equations

$$i\epsilon \sum_{p=1}^{N_H} (\phi_p, \phi_q) \mathrm{d}_t \hat{U}_p = \sum_{p=1}^{N_H} (\mathcal{H}\phi_p, \phi_q) \hat{U}_p \tag{3.20}$$

and

$$i\epsilon \sum_{p=1}^{N_H} (\hat{\phi}_p, \hat{\phi}_q) \mathrm{d}_t \hat{U}_p = \sum_{p=1}^{N_H} (\mathcal{H}\hat{\phi}_p, \hat{\phi}_q) \hat{U}_p. \tag{3.21}$$

If $\lambda = 0$, the two equations have the same solution with a given initial condition, while for $\lambda \neq 0$, the factor $(1, \phi_p^H)$ in the basis functions cannot be eliminated in the two sides of (3.21), and the two equations have different solutions. This issue can be addressed by the setup $\lambda(H) = (1, \phi_p^H)$.

Solving the optimal problems (3.15) on the fine mesh, we get

$$\phi_p = \sum_{s=1}^{N_h} c_p^s \phi_s^h, \quad p = 1, \cdots, N_H.$$

Define the MsFEM space $V_{ms} = span\{\phi_1, \cdots, \phi_{N_H}\}$, and it holds true that $V_{ms} \subset V_h$. Hence the solution of optimal problems defines a linear transformation $\mathcal{C} : V_h \mapsto V_{ms}$. On the other hand, the solution on the fine mesh can be reconstructed utilizing this linear mapping, which is essential in the formulation of the cubic nonlinear matrix. Note that the factor $\lambda(H)$ is a rescaling factor, and it doesn't change the basis function space. Thus we have the following propositions.

PROPOSITION 3.1 ([52], Lemma 3.2). *For all $\phi \in V_{ms}$ and $w \in W_h$, $a(\phi, w) = 0$ and $V_h = V_{ms} \oplus W_h$.*

Proof. As the same procedures in [52], we directly obtain $a(f, w) = 0, \forall f \in V_{ms}, w \in W_h$. For any $f \in V_h$, define

$$f^* = \sum_{p=1}^{N_H} \frac{(f, \phi_p^H)}{(1, \phi_p^H)} \phi_p.$$

Then $f^* \in V_{ms}$ and $(f - f^*, \phi_p^H) = 0$ for $p = 1, \cdots, N_H$. Thus $f - f^* \in W_h$ and we get the decomposition $V_h = V_{ms} \oplus W_h$. ∎

Due to $V_h = V_{ms} \oplus W_h$, W_h is also the kernel space of linear map $\mathcal{C}$. Furthermore, combining an iterative Caccioppoli-type argument [32, 36, 42, 44] and some refined assumption for the potential, and the multiscale finite element basis functions have the following exponential decaying property.

PROPOSITION 3.2 ([52], Theorem 3.2). *Under the resolution condition of the mesh size and potential, there exist positive constant C and $\beta \in (0, 1)$ independent of H, such that*

$$\|\nabla \phi_p\|_{L^2(\mathcal{D} \setminus D_\ell)} \leq C\beta^\ell \|\nabla \phi_p\|, \tag{3.22}$$

for all $p = 1, \cdots, N_H$.

By the multiscale basis functions, the weak form of the full NLSE reads as

$$(3.23)\quad i\epsilon\left(\sum_{p=1}^{N_H}\sum_{s=1}^{N_h}\mathrm{d}_t\hat{U}_p c_p^s\phi_s^h,\sum_{s=1}^{N_h}c_l^s\phi_s^h\right)=\frac{\epsilon^2}{2}\left(\sum_{p=1}^{N_H}\sum_{s=1}^{N_h}\hat{U}_p c_p^s\nabla\phi_s^h,\sum_{s=1}^{N_h}c_l^s\nabla\phi_s^h\right)$$

$$+\lambda\left(\left|\sum_{p=1}^{N_H}\sum_{s=1}^{N_h}\hat{U}_p c_p^s\phi_s^h\right|^2\sum_{p=1}^{N_H}\sum_{s=1}^{N_h}\hat{U}_p c_p^s\phi_s^h,\sum_{s=1}^{N_h}c_l^s\phi_s^h\right)$$

for all $l=1,\cdots,N_H$. The stiff matrix and mass matrix constructed by the multiscale basis functions satisfy $M^{ms}=\mathcal{C}^T M^h\mathcal{C}$ and $S^{ms}=\mathcal{C}^T S^h\mathcal{C}$. For the nonlinear term, the solution on the fine mesh is reconstructed by $\mathcal{C}\hat{U}$, and we then get the similar form $N^{ms}=\mathcal{C}^T N^h\mathcal{C}$. The construction of N^h suffers from heavy computation, especially for high-dimensional problems. And the application of time-splitting methods can avoid this issue. Thus we only need to solve linear equations at each time step, achieving high efficiency.

According to (3.18) and (3.19), the numerical solution on the coarse mesh can be denoted by $\{\hat{U}_p(t)\}_{p=1}^{N_H}$, while on the fine mesh denoted by $\left\{\sum_{p=1}^{N_H}\hat{U}_p(t)c_p^s\right\}_{s=1}^{N_h}$. For the sake of clarity, in the sequel, we denote the ψ_h^ϵ the classical FEM solution, and ψ_H^ϵ and $\psi_{H,h}^\epsilon$ the numerical solution constructed by the multiscale basis functions on the coarse mesh and fine mesh, respectively.

4. Convergence analysis.

4.1. Convergence analysis of the time-splitting FEM.

In this part, the **SI** is mainly considered and the L^2 error will be estimated. We start the convergence analysis from the temporal error estimate at the initial time step.

LEMMA 4.1. *If $\psi_{\mathrm{in}}\in H^4$, the error at the initial time step is bounded in the L^2 norm by*

$$\|\psi^\epsilon(\Delta t)-\psi^{\epsilon,1}\|=\|S^{\Delta t}\psi_{\mathrm{in}}-\mathcal{L}(\Delta t)\psi_{\mathrm{in}}\|\le C\|\psi_{\mathrm{in}}\|_{H^4}\frac{\Delta t^3}{\epsilon^3},$$

where C is a constant.

Proof. According to (3.5), we have

$$\psi^{\epsilon,1}=\exp\left(-\frac{i\Delta t}{2\epsilon}\mathcal{L}_2(\hat{\psi})-\frac{i\Delta t}{\epsilon}\mathcal{L}_1-\frac{i\Delta t}{2\epsilon}\mathcal{L}_2(\psi_{\mathrm{in}}^\epsilon)\right)\psi_{\mathrm{in}}^\epsilon$$

$$=\exp\left(-\frac{i\Delta t}{2\epsilon}\left(\mathcal{L}_2(\psi_{\mathrm{in}}^\epsilon)+\mathcal{O}(\frac{\Delta t^2}{\epsilon^2})\right)-\frac{i\Delta t}{\epsilon}\mathcal{L}_1-\frac{i\Delta t}{2\epsilon}\mathcal{L}_2(\psi_{\mathrm{in}}^\epsilon)\right)\psi_{\mathrm{in}}^\epsilon$$

$$=\exp\left(-\frac{i\Delta t}{\epsilon}\mathcal{L}_1-\frac{i\Delta t}{\epsilon}\mathcal{L}_2(\psi_{\mathrm{in}}^\epsilon)\right)\exp\left(-\frac{\Delta t^3}{\epsilon^3}\Gamma(2\mathcal{L}_1+\mathcal{L}_2)^2\right)\psi_{\mathrm{in}}^\epsilon,$$

where Γ depends on the form of $\mathcal{L}_2$. Use the expansion

$$\exp\left(-\frac{\Delta t^3}{\epsilon^3}\Gamma(2\mathcal{L}_1+\mathcal{L}_2)^2\right)=I-\frac{\Delta t^3}{\epsilon^3}\Gamma(2\mathcal{L}_1+\mathcal{L}_2)^2+\mathcal{O}\left(\frac{\Delta t^6}{\epsilon^6}\right)$$

and the dominant reminder has the form

$$\mathcal{R}_1^0=-\frac{\Delta t^3}{\epsilon^3}\Gamma(2\mathcal{L}_1+\mathcal{L}_2)^2\psi_{\mathrm{in}}^\epsilon.$$

Since the exact solution at $t = \Delta t$ is given by

$$\psi^\epsilon(\Delta t) = S^{\Delta t}\psi^\epsilon_{\text{in}} = \exp\left(-\frac{i\Delta t}{\epsilon}(\mathcal{L}_1 + \mathcal{L}_2(\psi^\epsilon_{\text{in}}))\right)\psi^\epsilon_{\text{in}}.$$

There exists a constant such that

$$\|\psi^\epsilon(\Delta t) - \psi^{\epsilon,1}\| \le C\|\psi^\epsilon_{\text{in}}\|_{H^4}\frac{\Delta t^3}{\epsilon^3}.$$

□

In turn, we prove the stability of the Strang splitting operator. Due to $\exp\left(-\frac{i\mathcal{L}_1 t}{\epsilon}\right)$ is unitary, for any $f_1,\ f_2 \in H^2$, we have

$$\left\|\exp\left(-\frac{i\mathcal{L}_1 t}{\epsilon}\right)f_1 - \exp\left(-\frac{i\mathcal{L}_1 t}{\epsilon}\right)f_2\right\| = \left\|\exp\left(-\frac{i\mathcal{L}_1 t}{\epsilon}\right)(f_1 - f_2)\right\| = \|f_1 - f_2\|.$$

Define $F(\psi) = -i\mathcal{L}_2(\psi)\psi$, the splitting solution for $\mathcal{L}_2$ is solved by the equation

$$\epsilon\partial_t\psi - F(\psi) = 0. \tag{4.1}$$

The nonlinear flow solved from this equation has the form

$$Y^t\psi = \psi + \frac{1}{\epsilon}\int_0^t F(Y^s\psi)\mathrm{d}s. \tag{4.2}$$

Assume that F is Lipschitz with a Lipschitz constant M, and repeat the proof in [11]. For all $f_1,\ f_2 \in L^2$, there exists a constant that depends on F such that for all $0 \le \tau \le 1$

$$\begin{aligned}\|Y^\tau f_1 - Y^\tau f_2\| &\le \|f_1 - f_2\| + \frac{1}{\epsilon}\int_0^\tau \|F(Y^s f_1) - F(Y^s f_2)\|\mathrm{d}s \\ &\le \|f_1 - f_2\| + \frac{M}{\epsilon}\int_0^\tau \|Y^s f_1 - Y^s f_2\|\mathrm{d}s.\end{aligned}$$

An application of the Gronwall lemma leads to

$$\|Y^\tau f_1 - Y^\tau f_2\| \le \exp\left(\frac{M\tau}{\epsilon}\right)\|f_1 - f_2\|. \tag{4.3}$$

In particular, for $F(\psi) = \lambda|\psi|^2\psi$ we get

$$\|\mathcal{L}(\tau)f_1 - \mathcal{L}(\tau)f_2\| \le \exp\left(\frac{M\lambda\tau}{\epsilon}\right)\|f_1 - f_2\|. \tag{4.4}$$

Besides, for the nonlinear flow (4.2), we have the following lemma.

LEMMA 4.2. *Let $\psi \in H^2$; if $F(\psi) = \lambda|\psi|^2\psi$, there exists a constant C such that for all* $0 \le \tau \le 1$

$$\|Y^\tau\psi\|_{H^2} \le \exp\left(\frac{\lambda\tau\|\psi\|^2_\infty}{\epsilon}\right)\|\psi\|_{H^2}. \tag{4.5}$$

If $F(\psi) = \lambda|\psi|^2\psi + v\psi$, there exists a constant C such that for $v \in H^2$ and for all $0 \le \tau \le 1$

$$\|Y^\tau\psi\|_{H^2} \le \exp\left(\frac{\tau(\|v\|_{H^2} + \lambda\|\psi\|^2_\infty)}{\epsilon}\right)\|\psi\|_{H^2}. \tag{4.6}$$

Proof. Consider $F(\psi) = \lambda|\psi|^2\psi + v\psi$. For the nonlinear flow (4.2), we have

$$\|Y^\tau\psi\|_\infty \le \|\psi\|_\infty + \frac{1}{\epsilon}\int_0^\tau \|F(Y^s\psi)\|_\infty \mathrm{d}s \le \|\psi\|_\infty + \frac{\|v\|_\infty + \lambda\|\psi\|_\infty^2}{\epsilon}\int_0^\tau \|Y^s\psi\|_\infty \mathrm{d}s.$$

Then the application of Gronwall inequality yields

$$\|Y^\tau\psi\|_\infty \le \exp\left(\frac{\tau(\|v\|_\infty + \lambda\|\psi\|_\infty^2)}{\epsilon}\right)\|\psi\|_\infty.$$

Similarly, for the H^2 norm, we directly have

$$\|Y^\tau\psi\|_{H^2} \le \|\psi\|_{H^2} + \frac{\|v\|_{H^2} + \lambda\|\psi\|_\infty^2}{\epsilon}\int_0^\tau \|Y^s\psi\|_{H^2}\mathrm{d}s,$$

which also leads to

$$\|Y^\tau\psi\|_{H^2} \le \exp\left(\frac{\tau(\|v\|_{H^2} + \lambda\|\psi\|_\infty^2)}{\epsilon}\right)\|\psi\|_{H^2}.$$

Let $v = 0$ and we get (4.5). This completes the proof. ∎

For the semi-discretized time-splitting methods, we have the convergence theorem of temporal accuracy.

THEOREM 4.3. *Let $\psi_{\text{in}} \in H^4$, $T > 0$ and $\Delta t \in (0, \epsilon)$. For $n\Delta t \le T$, there exists a constant C such that*

$$\|\mathcal{L}^n\psi_{\text{in}} - S^{n\Delta t}\psi_{\text{in}}\| \le CT\|\psi_{\text{in}}\|_{H^4}\left(1 + \frac{T}{\epsilon}\right)\frac{\Delta t^2}{\epsilon^3}. \tag{4.7}$$

Proof. Similar to the proof in [11, 17]. The triangle inequality yields

$$\|\mathcal{L}^n\psi_{\text{in}} - S^{n\Delta t}\psi_{\text{in}}\| \le \sum_{j=0}^{n-1}\|\mathcal{L}^{n-j}S^{j\Delta t}\psi_{\text{in}} - \mathcal{L}^{n-j-1}S^{(j+1)\Delta t}\psi_{\text{in}}\|.$$

Due to S^t being the Lie formula for all $t \le T$ and $\psi_{\text{in}} \in H^4$, $S^t\psi_{\text{in}}$ belongs to H^4 and is uniformly bounded in this space, thus for all j such that $j\Delta t \le T$, we have

$$\|\mathcal{L}S^{j\Delta t}\psi_{\text{in}} - S^{(j+1)\Delta t}\psi_{\text{in}}\| = \|(\mathcal{L} - S^{\Delta t})S^{j\Delta t}\psi_{\text{in}}\| \le C\|\psi_{\text{in}}\|_{H^4}\frac{\Delta t^3}{\epsilon^3}.$$

Combine with (4.4) and we get

$$\|\mathcal{L}^n\psi_{\text{in}} - S^{n\Delta t}\psi_{\text{in}}\| \le \sum_{j=0}^{n-1}\left(\exp\left(\frac{M\lambda\Delta t}{\epsilon}\right)\right)^{n-j-1}\|(\mathcal{L} - S^{\Delta t})S^{j\Delta t}\psi_{\text{in}}\|.$$

Since $0 < \Delta t < \epsilon$, for all $j \ge 0$, we have

$$\left(\exp\left(\frac{M\lambda\Delta t}{\epsilon}\right)\right)^j \le \left(1 + C_0\frac{\Delta t}{\epsilon}\right)^j \le 1 + Cj\frac{\Delta t}{\epsilon}.$$

Consequently, we arrive at

$$\|\mathcal{L}^n\psi_{\text{in}} - S^{n\Delta t}\psi_{\text{in}}\| \le \sum_{j=0}^{n-1}\left(\exp\left(\frac{M\lambda\Delta t}{\epsilon}\right)\right)^{n-j-1} C\|\psi_{\text{in}}\|_{H^4}\frac{\Delta t^3}{\epsilon^3}$$

$$\le C\|\psi_{\text{in}}\|_{H^4}\frac{\Delta t^3}{\epsilon^3}\sum_{j=0}^{n-1}\left(1 + C(n-j-1)\frac{\Delta t}{\epsilon}\right) \le CT\|\psi_{\text{in}}\|_{H^4}\left(1+\frac{T}{\epsilon}\right)\frac{\Delta t^2}{\epsilon^3}.$$

It concludes the proof of this theorem. ∎

Next, we give the convergence of the full TS-FEM method. Consider the problem

$$i\epsilon\partial_t\psi^\epsilon = \mathcal{L}_2\psi^\epsilon$$

with the initial condition ψ_{in} and the periodical boundary condition. The solution has the form

$$\psi^\epsilon(\boldsymbol{x}, t) = \exp\left(-\frac{it}{2\epsilon}\mathcal{L}_2\right)\psi_{\text{in}}. \tag{4.8}$$

If $\mathcal{L}_2$ consists of potential and nonlinear term, the regularity of $\psi^\epsilon(t, \boldsymbol{x})$ depends on the regularity of both the potential v and ψ_{in}, otherwise it only depends on ψ_{in}.

Assume that the numerical solution ψ_h^ϵ is given by (3.13) and $\psi^\epsilon(t_n) = S^{n\Delta t}\psi_{\text{in}}$ is the solution of (2.1). We write

$$\psi_h^{\epsilon,n} - \psi^\epsilon(t_n) = L^n\psi_h^0 - S^{n\Delta t}\psi_{\text{in}} = (L^n\psi_h^0 - \mathcal{L}^n\psi_{\text{in}}) + (\mathcal{L}^n\psi_{\text{in}} - S^{n\Delta t}\psi_{\text{in}}). \tag{4.9}$$

The first term denotes the error attributable to the space discretization and the second term is the splitting error of temporal discretization.

We first estimate the spatial error accommodation from $t = 0$ to $t = \Delta t$,

$$\psi_h^{\epsilon,1} - \psi^\epsilon(\Delta t) = L_2\left(\frac{\Delta t}{2}, \cdot\right) \circ L_1(\Delta t)L_2\left(\frac{\Delta t}{2}, \cdot\right) \circ \psi_h^0 - \mathcal{L}(\Delta t)\psi_{\text{in}}.$$

Let $\hat{\psi}_0 = \mathcal{L}_2(\frac{\Delta t}{2}, \cdot) \circ \psi_{\text{in}}$, and consider the problem

$$i\epsilon\partial_t\psi^\epsilon = -\frac{\epsilon^2}{2}\Delta\psi^\epsilon + v\psi^\epsilon \tag{4.10}$$

with the initial condition $\psi^\epsilon(t = 0) = \hat{\psi}_0$ and the periodical boundary condition. The corresponding weak form is

$$i\epsilon(\partial_t(\psi^\epsilon - \psi_h^\epsilon), \phi^h) = \frac{\epsilon^2}{2}(\nabla(\psi^\epsilon - \psi_h^\epsilon), \nabla\phi^h) + (v(\psi^\epsilon - \psi_h^\epsilon), \phi^h), \quad \forall\phi^h \in V_h. \tag{4.11}$$

Let $\psi^\epsilon - \psi_h^\epsilon = (\psi^\epsilon - R_h\psi^\epsilon) + \theta$, where $\theta = R_h\psi^\epsilon - \psi_h^\epsilon$ and $R_h\psi^\epsilon$ denotes the Ritz projection. According to (4.11), we get

$$i\epsilon(\partial_t[(\psi^\epsilon - R_h\psi^\epsilon) + \theta], \phi^h) = \frac{\epsilon^2}{2}(\nabla\theta, \nabla\phi^h) + (v(\psi^\epsilon - R_h\psi^\epsilon), \phi^h) + (v\theta, \phi^h). \tag{4.12}$$

Take $\phi^h = \theta$ in the above equation,

$$i\epsilon(\partial_t\theta, \theta) = -i\epsilon(\partial_t(\psi^\epsilon - R_h\psi^\epsilon), \theta) + \frac{\epsilon^2}{2}\|\nabla\theta\|^2 + (v(\psi^\epsilon - R_h\psi^\epsilon), \theta) + (v\theta, \theta),$$

and we have

$$i\epsilon \mathrm{d}_t\|\theta\|^2 = i\epsilon(\partial_t\theta,\theta) + i\epsilon(\partial_t\bar{\theta},\bar{\theta}) = 2i\epsilon\Re(\partial_t(\psi^\epsilon - R_h\psi^\epsilon),\theta) + 2i\Im(v(\psi^\epsilon - R_h\psi^\epsilon),\theta),$$

which induces

$$\mathrm{d}_t\|\theta\| \le 2\|\partial_t(\psi^\epsilon - R_h\psi^\epsilon)\| + \frac{2}{\epsilon}\|v\|_\infty\|\psi^\epsilon - R_h\psi^\epsilon\|. \tag{4.13}$$

Integrating from 0 to t yields

$$\|\theta(t)\| \le \|\theta(0)\| + 2\int_0^t \|\partial_t(\psi^\epsilon - R_h\psi^\epsilon)\|\mathrm{d}t + \frac{2}{\epsilon}\|v\|_\infty \int_0^t \|\psi^\epsilon - R_h\psi^\epsilon\|\mathrm{d}t. \tag{4.14}$$

Assume $\|\theta(0)\| = \|\hat{\psi}_{\mathrm{in}} - R_h\hat{\psi}_{\mathrm{in}}\| = \|\psi_{\mathrm{in}} - R_h\psi_{\mathrm{in}}\| = 0$. Since $\|R_h\partial_t\psi^\epsilon - \partial_t\psi^\epsilon\| \le Ch^2\|\partial_t\psi^\epsilon\|_{H^2}$, we have

$$\|\theta(t)\| \le Cth^2\|\partial_t\psi^\epsilon\|_{H^2} + \frac{Ch^2}{\epsilon}\int_0^t \|\psi^\epsilon\|_{H^2}\mathrm{d}s \le C_{\lambda,\epsilon}th^2 + \frac{Cth^2}{\epsilon^3} \le CC_{\lambda,\epsilon}th^2, \tag{4.15}$$

where $t \le \Delta t$, and $C_{\lambda,\epsilon}$ is the leading order term with respect to ϵ^{-1}.

Let $\hat{\psi}_{h,1}$ be the numerical solution of (4.10) with $t = \Delta t$, we can obtain

$$\begin{aligned}\|\psi_h^{\epsilon,1} - \psi^\epsilon(\Delta t)\| &= \left\|\exp\left(-\frac{i\Delta t\mathcal{L}_2(\hat{\psi}_{h,1})}{2\epsilon}\right)\hat{\psi}_{h,1} - \exp\left(-\frac{i\Delta t\mathcal{L}_2(\hat{\psi}_1)}{2\epsilon}\right)\hat{\psi}_1\right\| \\ &\le C\exp\left(\frac{M\lambda\Delta t}{2\epsilon}\right)\|\theta(t)\|,\end{aligned}$$

where $\hat{\psi}_1 = \exp\left(-\frac{i\epsilon\Delta t\mathcal{L}_1}{\epsilon}\right)\exp\left(-\frac{i\epsilon\Delta t\mathcal{L}_2}{2\epsilon}\right)\psi_{\mathrm{in}}$. This indicates the spatial error accumulation in a one-time step. We next estimate the error accumulation in both time and space from $t = 0$ to T.

THEOREM 4.4. *Assume that $\psi_h^{\epsilon,n} = L^n\psi_{\mathrm{in}}$ and $\psi^\epsilon(n\Delta t) = S^{n\Delta t}\psi_{\mathrm{in}}$ are the numerical solution and exact solution of the NLSE. Assume $\partial_t\psi^\epsilon \in H^2$ for all $t \in [0,T]$ and $\psi_{\mathrm{in}} \in H^4$, then fora given $T > 0$, there exists a constant h_0 such that $h \le h_0$ and for all $\Delta t < \epsilon$ with $n\Delta t \le T$, and the L^2 error estimate satisfies*

$$\|\psi_h^{\epsilon,n} - \psi^\epsilon(n\Delta t)\| \le CC_{\lambda,\epsilon}h^2 + CT\left(1 + \frac{T}{\epsilon}\right)\frac{\Delta t^2}{\epsilon^3}, \tag{4.16}$$

where the constant C is independent of ϵ and T.

Proof. The error can be split into

$$\psi_h^{\epsilon,n} - \psi^\epsilon(n\Delta t) = L^n\psi_h^0 - S^{n\Delta t}\psi_{\mathrm{in}} = (L^n\psi_h^0 - \mathcal{L}^n\psi_{\mathrm{in}}) + (\mathcal{L}^n\psi_{\mathrm{in}} - S^{n\Delta t}\psi_{\mathrm{in}}).$$

The first term on the right-hand side satisfies

$$\|L^n\psi_h^0 - \mathcal{L}^n\psi_{\mathrm{in}}\| \le \left\|\sum_{j=1}^n L^{n-j}(LR_h - R_h\mathcal{L})\mathcal{L}^{j-1}\psi_{\mathrm{in}}\right\| + \|(R_h - I)\mathcal{L}^n\psi_{\mathrm{in}}\|.$$

Due to $\mathcal{L}_1$ conserving the H^2 norm of the solution and Lemma 4.2, we have $\mathcal{L}^n\psi_{\mathrm{in}} \in H^2$ and $\|(R_h - I)\mathcal{L}^n\psi_{\mathrm{in}}\| \le Ch^2\|\mathcal{L}^n\psi_{\mathrm{in}}\|_{H^2}$. Meanwhile,

$$\|L\psi^\epsilon\| \le \|L\psi^\epsilon - \mathcal{L}(\Delta t)\psi^\epsilon\| + \|\mathcal{L}(\Delta t)\psi^\epsilon\| \le CC_{\lambda,\epsilon}\Delta th^2 + \|\psi^\epsilon\|.$$

Similar to the Theorem 3.1 in [5], we denote the bound of the numerical solution by

$$\max_{1\le m\le n} \|L^m R_h \mathcal{L}^{n-m}\psi^\epsilon\| \le a_L.$$

Recall (4.14)-(4.15), owing to $\Delta t < \epsilon$, then there exists a constant C independent of ϵ such that

$$\left\|\sum_{j=1}^{n} L^{n-j}(LR_h - R_h\mathcal{L})\mathcal{L}^{j-1}\psi_{\text{in}}\right\| \le n\exp\left(CTa_L^2\right)\max_{1\le j\le n}\|(LR_h - R_h\mathcal{L})\mathcal{L}^{j-1}\psi_{\text{in}}\|$$

$$\le n\exp\left(CTa_L^2\right)\exp\left(\frac{\lambda M\Delta t}{\epsilon}\right)CC_{\lambda,\epsilon}\Delta t h^2 \le \exp\left(CTa_L^2\right)\exp\left(\frac{\lambda M\Delta t}{\epsilon}\right)CC_{\lambda,\epsilon}Th^2.$$

Thus we arrive at

$$\|L^n\psi_{\text{in}} - \mathcal{L}^n\psi_{\text{in}}\| \le CC_{\lambda,\epsilon}h^2,$$

where C is independent of ϵ but depends on T and λ. Note that the order of $\|\psi^\epsilon\|_{H^2}$ with respect to ϵ^{-1} is lower than $C_{\lambda,\epsilon}$, and it is ignored in this results.

Furthermore, combine with Theorem 4.3, and we get the desired estimate

$$\begin{aligned}\|\psi_h^{\epsilon,n} - \psi^\epsilon(n\Delta t)\| &\le \|L^n\psi_{\text{in}} - \mathcal{L}^n\psi_{\text{in}}\| + \|\mathcal{L}^n\psi_{\text{in}} - S^{n\Delta t}\psi_{\text{in}}\| \\ &\le CC_{\lambda,\epsilon}h^2 + CT\left(1+\frac{T}{\epsilon}\right)\frac{\Delta t^2}{\epsilon^3}.\end{aligned}$$

This declares the (4.16). ∎

Remark 4.5. Take a further simplification

$$\frac{C}{\epsilon^3}\left(1+\frac{T}{\epsilon}\right) \le \frac{CT}{\epsilon^4}.$$

We temporarily use $\psi_H^{\epsilon,n}$ to denote the FEM solution on the coarse mesh with mesh size H, the counterpart result of Theorem 4.4 on the coarse space is

$$\|\psi_H^{\epsilon,n} - \psi^\epsilon(n\Delta t)\| \le CC_{\lambda,\epsilon}H^2 + \frac{CT^2}{\epsilon^4}\Delta t^2. \tag{4.17}$$

Here we obtain the L^2 error estimate of the TS-FEM for the deterministic NLSE. Next, the convergence analysis of the MsFEM in space, accompanied by the qMC method, will be further assessed. Note that the convergence analysis of the TS-FEM with the qMC method is similar, thus we will not discuss it in the subsequent section.

4.2. Convergence analysis of the TS-MsFEM for NLSE with random potentials. In this part, we first give the convergence analysis of the TS-MsFEM for the NLSE with the deterministic potential. Secondly, employing the qMC method in the random space, we further obtain the error estimate of the TS-MsFEM for the NLSE with random potentials.

4.2.1. TS-MsFEM for the deterministic NLSE. For **SI**, we solve the linear Schrödinger equation by the MsFEM, and the corresponding convergence analysis has been given in [52]. We therefore have the following estimate.

LEMMA 4.6. *Let $\psi_H^{\epsilon,n} = L_{ms}^n \psi_{\rm in}$ be the numerical solution solved in V_{ms} by* **SI**, *and $\psi^\epsilon(t_n) = S^{n\Delta t}\psi_{\rm in}$ be the exact solution of the NLSE. Let $\Delta t \in (0,\epsilon)$, and assume $\partial_t \psi^\epsilon \in L^2$ for all $t \in (0,T]$, and $\psi_{\rm in} \in H^4$. We have the estimate*

$$\|\psi_H^{\epsilon,n} - \psi^\epsilon(t_n)\| \le \frac{CTH^2}{\epsilon^3} + \frac{CT^2}{\epsilon^4}\Delta t^2, \tag{4.18}$$

where the constant C is independent of ϵ.

Proof. For the linear Schrödinger equation, the spatial error of multiscale solution and exact solution has the bound [52]

$$\|\psi_H^\epsilon - \psi^\epsilon\| \le \frac{CH^2}{\epsilon^2}\|\epsilon\partial_t\psi^\epsilon\| \le \frac{CH^2}{\epsilon}\|\partial_t\psi_{\rm in}\| \exp\left(\frac{2\lambda t\|\psi^\epsilon\|_\infty^2}{\epsilon}\right).$$

At the second step of **SI**, we have

$$\|\psi_H^\epsilon - \psi^\epsilon\| \le \frac{CH^2}{\epsilon^2}\exp\left(\frac{2\lambda\Delta t\|\psi^\epsilon\|_\infty^2}{\epsilon}\right) \le \frac{CH^2}{\epsilon^2}.$$

When the eigendocomposition method is applied, the solution can be solved exactly in time for linear problems. The accumulation of the spatial error at each time step satisfies

$$\begin{aligned}&\|L_{ms}\psi_H^{\epsilon,n} - \mathcal{L}\psi^{\epsilon,n}\| \le \|L_{ms}\psi_H^{\epsilon,n} - \mathcal{L}I_H\psi^{\epsilon,n}\| + \|\mathcal{L}I_H\psi^{\epsilon,n} - \mathcal{L}\psi^{\epsilon,n}\|\\ &\le \exp\left(\frac{\lambda M\Delta t}{2\epsilon}\right)\frac{CH^2}{\epsilon^2} + \exp\left(\frac{\lambda M\Delta t}{\epsilon}\right)\|I_H\psi^{\epsilon,n} - \psi^{\epsilon,n}\| \le \exp\left(\frac{\lambda M\Delta t}{\epsilon}\right)\frac{CH^2}{\epsilon^2}.\end{aligned}$$

Meanwhile, by the Strang splitting method, repeat the procedures in Theorem 4.3, and we get the estimate as (4.18). ∎

Remark 4.7. In comparison to Remark 4.5, the MsFEM exhibits a superior bound on ϵ, as it requires only the bound $\|\partial_t\psi^\epsilon\|$. In contrast, the application of the classical FEM requires the bound of $\|\partial_t\psi^\epsilon\|_{H^2}$, which implies a high-order dependence on ϵ. Consequently, the weak dependence of MsFEM on ϵ demonstrates its superiority in handling multiscale problems effectively.

4.2.2. MsFEM for the NLSE with random potentials. To carry out the convergence analysis for the qMC method, the regularity of the wave function with respect to random variables is required. Since the random potential is truncated by the m-order KL expansion, we denote $\boldsymbol{\xi}(\omega) = (\xi_1(\omega), \cdots, \xi_m(\omega))^T$. Let $\boldsymbol{\nu} = (\nu_1, \cdots, \nu_m)$ be the multi-index with ν_j being the nonnegative integer, where $|\boldsymbol{\nu}| = \sum_{j=1}^m \nu_j$. Then $\partial^{\boldsymbol{\nu}}\psi_m^\epsilon$ denotes the mixed derivative of ψ_m^ϵ with respect to all random variables specified by the multi-index $\boldsymbol{\nu}$.

LEMMA 4.8. *For any $\omega \in \Omega$ and multi-index $|\boldsymbol{\nu}| < \infty$, and for all $t \in (0,T]$, there exists a constant $C(T,\lambda,\epsilon,|\boldsymbol{\nu}|)$ depends on $T,\lambda,\epsilon,|\boldsymbol{\nu}|$ such that the partial derivative of $\psi_m^\epsilon(t,\boldsymbol{x},\omega)$ satisfies the priori estimate*

$$\|\partial^{\boldsymbol{\nu}}\psi_m\|_{H^2} \le C(T,\lambda,\epsilon,|\boldsymbol{\nu}|)\prod_j(\sqrt{\lambda_j}\|v_j\|_{H^2})^{\nu_j}. \tag{4.19}$$

The proof of this lemma is given in the appendix.

We are interested in the expectation of linear functionals of the numerical solution in applications of uncertainty quantification. Here for the NLSE with random potentials, we will estimate the expected value $\mathbb{E}[\mathcal{G}(\psi_m^\epsilon(\cdot,\omega)]$ of the random variable $\mathcal{G}(\psi_m^\epsilon(\cdot,\omega))$. Let $\mathcal{G}(\cdot)$ be a continuous linear functional on $L^2(\mathcal{D})$, then there exists a constant $C_\mathcal{G}$ such that

$$|\mathcal{G}(u)| \leq C_\mathcal{G}\|u\|$$

for all $u \in L^2(\mathcal{D})$. Consider the integral

$$I_m(F) = \int_{\boldsymbol{\xi}\in[0,1]^m} F(\boldsymbol{\xi})\mathrm{d}\boldsymbol{\xi}, \tag{4.20}$$

where $F(\boldsymbol{\xi}) = \mathcal{G}(\psi_m^\epsilon(\cdot,\boldsymbol{\xi}))$. To approximate this integral, both the MC and qMC can be used. In our methods, it is approximated over the unit cube by randomly shifted lattice rules

$$Q_{m,n}(\boldsymbol{\Delta};F) = \frac{1}{N}\sum_{i=1}^{N} F\left(frac\left(\frac{iz}{N}+\boldsymbol{\Delta}\right)\right),$$

where $z \in \mathbb{N}^m$ is the generating vector and $\boldsymbol{\Delta} \in [0,1]^m$. Here N denotes the number of random samples.

LEMMA 4.9. *For the integral* (4.20)*, given $m, N \in \mathbb{N}$ with $N \leq 10^{30}$, weights $\gamma = (\gamma_\mathbf{u})_{\mathbf{u}\subset\mathbb{N}}$, a randomly shifted lattice rule with N points in m dimensional random space could be constructed by a component-by-component such that for all $\alpha \in (\frac{1}{2}, 1]$*

$$\sqrt{\mathbb{E}^{\boldsymbol{\Delta}}|I_m(F) - Q_{m,N}(\cdot;F)|} \leq 9C^*C_{\gamma,m}(\alpha)N^{-1/2\alpha},$$

where

$$C_{\gamma,m}(\alpha) = \left(\sum_{\emptyset\neq\mathbf{u}\subseteq\{1:m\}} \gamma_\mathbf{u}^\alpha \prod_{j\in\mathbf{u}} \varrho(\alpha)\right)^{1/2\alpha} \left(\sum_{\mathbf{u}\subseteq\{1:m\}} \frac{(C(\boldsymbol{\nu}))^2}{\gamma_\mathbf{u}} \prod_{j\in\mathbf{u}} \lambda_j\|v_j\|_{H^2}^2\right)^{1/2}.$$

Proof. The proof of the lemma is the same as in [15]. Here $C(\boldsymbol{\nu}) = C(t,\lambda,\epsilon,|\boldsymbol{\nu}|)$ is calculated in Lemma 4.8. And

$$\varrho(\alpha) = 2\left(\frac{\sqrt{2\pi}}{\pi^{2-2\eta_*(1-\eta_*)\eta_*}}\right)^\alpha \zeta\left(\alpha+\frac{1}{2}\right), \tag{4.21}$$

where $\eta_* = \frac{2\alpha-1}{4\alpha}$, $\zeta(x)$ is the Riemann zeta function and $C^* = \|\mathcal{G}\|$. The details of these estimates can be found in [18, 26]. ∎

Employing the qMC sampling, the estimate between the wave functions of (2.1) and the truncated NLSE (2.10) satisfies the following lemma.

LEMMA 4.10. *Under the Assumption* 2.2*, there exists a constant C such that*

$$\sqrt{\mathbb{E}^{\boldsymbol{\Delta}}[|\mathbb{E}[\mathcal{G}(\psi^\epsilon)] - Q_{m,N}[\mathcal{G}(\psi_m^\epsilon)]|^2]} \leq C\left(\frac{m^{-\chi}}{\epsilon} + C_{\gamma,m}N^{-r}\right), \tag{4.22}$$

where $0 \leq \chi \leq (\frac{1}{2}-\eta)\Theta - \frac{1}{2}$, $r = 1-\delta$ for $0 < \delta < \frac{1}{2}$. Note that the constant C is independent of m and n but depends on T.

Proof. Since $\mathcal{G}$ is a linear functional, we have

$$\begin{aligned}|\mathbb{E}[\mathcal{G}(\psi^\epsilon)] - Q_{m,N}[\mathcal{G}(\psi^\epsilon_m)]| &\le |\mathbb{E}[\mathcal{G}(\psi^\epsilon)] - I_m(\psi^\epsilon)| + |I_m(\psi^\epsilon) - Q_{m,N}[\mathcal{G}(\psi^\epsilon_m)]| \\ &= |\mathbb{E}[\mathcal{G}(\psi^\epsilon)] - \mathbb{E}[\mathcal{G}(\psi^\epsilon_m)]| + |I_m(\psi^\epsilon) - Q_{m,N}[\mathcal{G}(\psi^\epsilon_m)]|.\end{aligned}$$

The first term satisfies

$$|\mathbb{E}[\mathcal{G}(\psi^\epsilon)] - \mathbb{E}[\mathcal{G}(\psi^\epsilon_m)]| \le \mathbb{E}[|\mathcal{G}(\psi^\epsilon) - \mathcal{G}(\psi^\epsilon_m)|] \le C\frac{m^{-\chi}}{\epsilon},$$

where C depends on the time T. Let $\alpha = 1/(2-2\delta)$ for $0 < \delta < \frac{1}{2}$, according to Lemma 4.9, we then get

$$\begin{aligned}&\mathbb{E}^{\boldsymbol{\Delta}}[|\mathbb{E}[\mathcal{G}(\psi^\epsilon)] - Q_{m,N}[\mathcal{G}(\psi^\epsilon_m)]|^2] \\ \le&\mathbb{E}^{\boldsymbol{\Delta}}[|\mathbb{E}[\mathcal{G}(\psi^\epsilon)] - I_m(\psi^\epsilon)|^2] + \mathbb{E}^{\boldsymbol{\Delta}}[|I_m(\psi^\epsilon) - Q_{m,N}[\mathcal{G}(\psi^\epsilon_m)]|^2] \\ \le&C\frac{m^{-2\chi}}{\epsilon^2} + CC^2_{\gamma,m}N^{2-2\delta}.\end{aligned}$$

∎

Employ the qMC method in the random space, for the numerical solution $\psi_H^{\epsilon,m}$ solved by MsFEM on the coarse mesh, then we have the following error estimate.

THEOREM 4.11. *Let $\psi_{\text{in}} \in H^4(\mathcal{D})$, $\psi^\epsilon \in L^\infty([0,T]; H^4(\mathcal{D})) \cap L^1([0,T]; H^2(\mathcal{D}))$, and parameterized potentials satisfy the Assumption 2.2. Consider $\mathbb{E}[\mathcal{G}(\psi^\epsilon(t_n))]$ is approximated by $Q_{m,N}(\cdot; \mathcal{G}(\psi^{\epsilon,n}_{H,m}))$. Apply the random shifted lattice rule $Q_{m,N}$ to $\mathcal{G}(\psi^\epsilon(t_n))$. Then for any fixed $T > 0$, there exists a constant H_0 such that $H \le H_0$ and for all $\Delta t < \epsilon$ with $n\Delta t \le T$, we have the root-mean-square error as*

(4.23)
$$\sqrt{\mathbb{E}^{\boldsymbol{\Delta}}[|\mathbb{E}[\mathcal{G}(\psi^\epsilon(t_n))] - Q_{m,N}[\mathcal{G}(\psi^{\epsilon,n}_{H,m})]|^2]} \le C\left(\frac{H^2}{\epsilon^3} + \frac{\Delta t^2}{\epsilon^4} + \frac{m^{-\chi}}{\epsilon} + C_{\gamma,m}N^{-r}\right),$$

where $0 \le \chi \le (\frac{1}{2} - \eta)\Theta - \frac{1}{2}$, and $r = 1 - \delta$ for $0 < \delta < \frac{1}{2}$. Here C is independent of m and N but depends on λ and T, and $C_{\gamma,m}$ depends on T, λ and ϵ.

Proof. We split the error (4.23) into

$$\begin{aligned}|\mathbb{E}[\mathcal{G}(\psi^\epsilon(t_n))] - Q_{m,N}[\mathcal{G}(\psi^{\epsilon,n}_{H,m})]| \le&|\mathbb{E}[\mathcal{G}(\psi^\epsilon(t_n))] - Q_{m,N}[\mathcal{G}(\psi^\epsilon_m(t_n))]| \\ &+ |Q_{m,N}[\mathcal{G}(\psi^\epsilon_m(t_n))]] - Q_{m,N}[\mathcal{G}(\psi^{\epsilon,n}_{H,m})]|.\end{aligned}$$

The second term can be estimated by

$$|\mathcal{G}(\psi^\epsilon_m(t_n)) - \mathcal{G}(\psi^{\epsilon,n}_{H,m})| \le C_{\mathcal{G}}\|\psi^\epsilon_m(t_n) - \psi^{\epsilon,n}_{H,m}\| \le CC_{\mathcal{G}}\left(\frac{H^2}{\epsilon^3} + \frac{\Delta t^2}{\epsilon^4}\right),$$

where the constant C depends on λ and T, and is independent of m and N. Combine with Lemma 4.10, we get the (4.23). This completes this proof. ∎

Remark 4.12. Theorem 4.11 gives the L^2 estimate of TS-MsFEM for the NLSE with random potentials. For the employment of the TS-FEM, repeat the above procedures and we can get a similar result.

In the proposed methods, when accounting for random potentials, constructing multiscale basis functions demands substantial computational cost as the number of samples grows. To improve the simulation efficiency, we propose a multiscale reduced basis method consisting of offline and online stages. In the offline stage, we utilize the proper orthogonal decomposition (POD) method to derive a small set of multiscale reduced basis functions of random space. Using these random basis functions, we simplify the optimal problems in the online stage to construct basis functions. This method is detailed in Appendix A.

5. Numerical experiments.

In this part, we will present numerical experiments in both 1D and 2D physical space. The convergence rates of TS-FEM and TS-MsFEM are first verified. For the NLSE with the random potential, we compare the convergence rate in the random space. In addition, the delocalization of mass distribution due to disordered potentials and the cubic nonlinearity is investigated.

5.1. Numerical accuracy of TS-FEMs.

Set $\psi_{\text{in}}(x) = (10\pi)^{0.25}\exp(-20x^2)$ for the 1D case, and $\psi_{\text{in}}(x_1, x_2) = (10/\pi)^{0.25}\exp(-5(x_1-0.5)^2 - 5(x_2-0.5)^2)$ for the 2D case. To begin with, we choose the harmonic potential $v(x) = 0.5x^2$, and verify the second-order accuracy of the TS-FEM with respect to the temporal step size Δt and spatial mesh size h. Here we fix the terminal time $T = 1.0$, $\epsilon = \frac{1}{16}$ and nonlinear parameter $\lambda = 0.1$. The reference solution $\psi^\epsilon_{\text{ref}}$ is computed on the fine mesh with $h = \frac{2\pi}{2048}$ and $\Delta t = 1.0\text{e-}06$. The L^2 absolute error and H^1 absolute error are recorded in Table 1.

Table 1: Numerical convergence of TS-FEMs in space and time.

	h	$\frac{2\pi}{128}$	$\frac{2\pi}{256}$	$\frac{2\pi}{512}$	$\frac{2\pi}{1024}$	order
SI	L^2 error	1.96e-02	5.22e-03	1.26e-03	2.54e-04	2.09
	H^1 error	1.19e-01	3.36e-02	8.31e-03	1.68e-04	2.04
SII	L^2 error	3.04e-02	8.07e-03	1.95e-03	3.92e-04	2.09
	H^1 error	3.52e-01	9.95e-02	2.44e-02	4.92e-03	2.05

	Δt	4.0e-02	2.0e-02	1.0e-02	5.0e-03	order
SI	L^2 error	4.53e-04	1.13e-04	2.81e-05	7.03e-06	2.00
	H^1 error	2.09e-03	5.20e-04	1.30e-04	3.24e-05	2.00
SII	L^2 error	7.16e-03	1.87e-03	4.71e-04	1.18e-04	1.98
	H^1 error	1.12e-01	2.91e-02	7.26e-03	1.81e-03	1.99

For the 2D case, we employ the multiscale potential

$$v(x_1, x_2) = \cos\left(x_1 x_2 + \frac{x_1}{\epsilon} + \frac{x_1 x_2}{\epsilon^2}\right), \tag{5.1}$$

over $\mathcal{D} = [0,1]^2$ with 64×64 spatial nodes. Here we set $\lambda = 1.0$ and multiscale coefficient $\epsilon = \frac{1}{8}$. We compare the numerical solution with the different Δt for **SI** and **SII**. By the means of the numerical tests shown in Figure 1, **SI** allows a bigger time step size than **SII**.

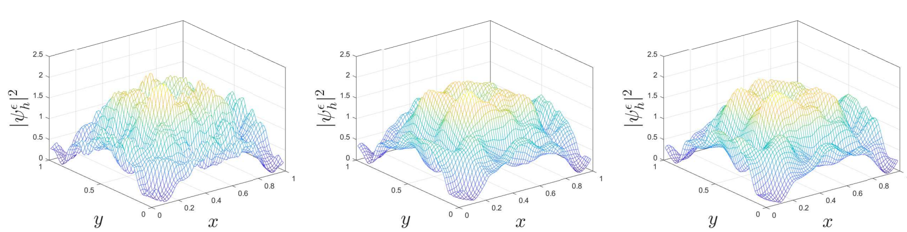

(a) **SI**, $\Delta t = 1.0\text{e-}02$ (b) **SI**, $\Delta t = 1.0\text{e-}03$. (c) **SII**, $\Delta t = 1.0\text{e-}03$.

Fig. 1: Numerical solution computed by the two TS-FEMs with different Δt.

5.2. Numerical experiments of TS-MsFEMs. Here the multiscale solution has two forms: ψ_H^ϵ on the coarse mesh and $\psi_{H,h}^\epsilon$ on the fine mesh. We first employ the harmonic potential. We vary the values of H and record the error between the numerical solution and the reference solution in Table 2. The parameters of this simulation are: $\lambda = 0.1$, $\epsilon = \frac{1}{16}$, $T = 1.0$, Δt =1.0e-03 and the fine mesh size $h = \frac{2\pi}{4096}$. It is shown that **SI** achieves the second-order convergence rate in both the coarse and fine spaces. The superconvergence is exhibited in coarse space for **SII**.

Table 2: Numerical convergence rate of the TS-MsFEMs for the NLSE with harmonic potential in space.

	H	$\|\psi_{H,h}^\epsilon - \psi_{\mathrm{ref}}^\epsilon\|$	$\|\psi_{H,h}^\epsilon - \psi_{\mathrm{ref}}^\epsilon\|_{H^1}$	$\|\psi_H^\epsilon - \psi_{\mathrm{ref}}^\epsilon\|$	$\|\psi_H^\epsilon - \psi_{\mathrm{ref}}^\epsilon\|_{H^1}$
SI	$2h$	4.95e-05	4.69e-04	3.47e-05	3.31e-04
	$4h$	1.68e-04	1.60e-03	1.18e-04	1.13e-03
	$8h$	6.44e-04	6.11e-03	4.52e-04	4.32e-03
	$16h$	2.56e-03	2.43e-02	1.80e-03	1.72e-02
	order	1.90	1.90	1.90	1.90
SII	$2h$	1.79e-05	1.73e-04	5.43e-12	1.88e-10
	$4h$	6.10e-05	5.86e-04	7.85e-11	1.63e-09
	$8h$	2.33e-04	2.24e-03	5.68e-09	1.02e-07
	$16h$	9.24e-04	8.89e-03	4.49e-07	8.24e-06
	order	1.90	1.90	5.52	5.22

Furthermore, to demonstrate the advantage of Option 1, we consider the discontinuous potential as shown in Figure 2. The second-order spatial convergence rate of **SI** is maintained, while the convergence rate of **SII** degenerates.

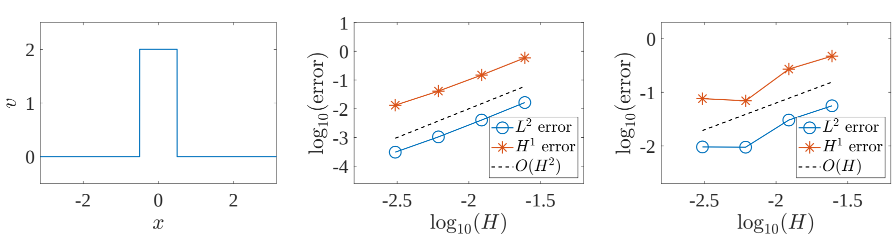

(a) $v(\boldsymbol{x})$. (b) **SI**. (c) **SII**.

Fig. 2: Numerical convergence rate of **SI** and **SII** for the discontinuous potential. In the plots, the L^2 error and H^1 error on the coarse mesh are depicted.

For the 2D case, we consider the discontinuous checkboard potential

$$v_2 = \begin{cases} \left(\cos\left(2\pi\frac{x_1}{\epsilon_2}\right)+1\right)\left(\cos\left(2\pi\frac{x_2}{\epsilon_2}\right)+1\right), & \{0 \le x_1, x_2 \le 0.5\} \cup \{0.5 \le x_1, x_2 \le 1\}, \\ \left(\cos\left(2\pi\frac{x_1}{\epsilon_1}\right)+1\right)\left(\cos\left(2\pi\frac{x_2}{\epsilon_1}\right)+1\right), & \text{otherwise}, \end{cases}$$

where $v = v_1 + v_2$ with $v_1 = |x_1 - 0.5|^2 + |x_2 - 0.5|^2$, $\epsilon_1 = \frac{1}{8}$ and $\epsilon_2 = \frac{1}{6}$. In the simulations, we set $h = \frac{1}{128}$, $\epsilon = \frac{1}{4}$, $\lambda = 1.0$, Δt =1.0e-04 and $T = 1.0$. We employ

SI (Figure 3) and **SII** (Figure 4) for time evolving. We vary the coarse mesh size with $H = 4h$ and $H = 8h$ of the MsFEM, and present the corresponding spatial error distribution. Here the reference solution is calculated using the FEM with a mesh size of h. In both Figure 3 and Figure 4, a substantial error is evident for the MsFEM with the mesh size ratio $H = 8h$. However, the numerical solution computed by the MsFEM still outperforms the results computed by the FEM with the same mesh size. Furthermore, this simulation highlights the superior performance of **SI** when dealing with discontinuous potentials.

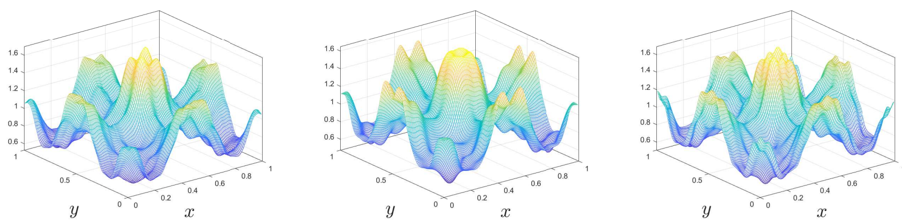

(a) Numerical solution computed by FEM, MsFEM with $H = 8h$ and MsFEM with $H = 4h$.

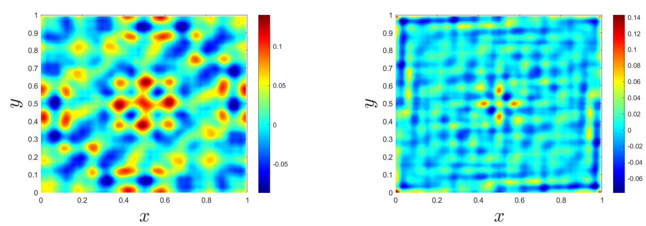

(b) Spatial error distribution of MsFEM with $H = 8h$ and $H = 4h$.

Fig. 3: Numerical solution and the corresponding spatial error distribution computed by **SI**, in which the FEM and MsFEM are used for spatial discretization.

5.3. Numerical simulations of NLSE with random potentials. For the 1D case, we consider the random potential

$$v(x, \omega) = \sigma \sum_{j=1}^{m} \sin(jx) \frac{1}{j^{\beta}} \xi_j(\omega), \tag{5.2}$$

where σ controls the strength of randomness, and $\xi_j(\omega)$'s are mean-zero and i.i.d random variables uniformly distributed in $[-\sqrt{3}, \sqrt{3}]$. It is extended to 2D as

$$v(x_1, x_2, \omega) = \sigma \sum_{j=1}^{m} \sin(jx_1) \sin(jx_2) \frac{1}{j^{\beta}} \xi_j(\omega). \tag{5.3}$$

For comparison, we employ the MC method and qMC method to generate the samples $\xi_j(\omega)$ in the simulations. And we measure the states of the system by the expectation of mass density

$$\mathbb{E}(|\psi^{\epsilon}_{H,h}|^2) = \frac{1}{N} \sum_{i} |\psi^{\epsilon}_{H,h}(\omega_i)|^2,$$

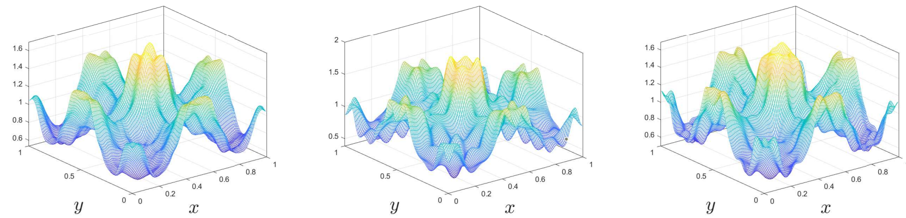

(a) Numerical solution computed by FEM, MsFEM with $H = 8h$ and MsFEM with $H = 4h$.

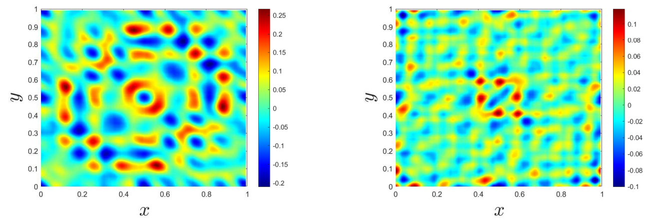

(b) Error distribution in space of MsFEM with $H = 8h$ and $H = 4h$.

Fig. 4: Numerical solution and the corresponding spatial error distribution computed by **SII**, in which the FEM and MsFEM are used for spatial discretization.

where N denotes the number of MC or qMC samples. To observe the evolution in the mass distribution of the system, we introduce the definition

$$A(t) = \mathbb{E}\left(\int_{\mathcal{D}} |\mathbf{x}|^2 |\psi^\epsilon|^2 \mathrm{d}\mathbf{x}\right), \tag{5.4}$$

which is extensively used to indicate the Anderson localization of the Schrödinger equation with random potentials.

5.3.1. Comparison of FEM and MsFEM. We set $\sigma = 1.0$, $\beta = 0$ and $m = 5$ in (5.2), and the number of qMC samples to be 500. The multiscale parameter is $\epsilon = \frac{1}{8}$, and the computational domain is $\mathcal{D} = [-2, 2]$. For the TS-FEMs, the solution is computed on the fine mesh with $h = \frac{2\pi}{600}$, and we set $H = 6h$ for the TS-MsFEMs. The terminal time is set to be $T = 10$. As shown in Figure 5, we show the evolution of $A(t)$ and $\mathbb{E}(|\psi^\epsilon_{H,h}|^2)$ at $T = 10$. The localization of linear Schrödinger equation and weak delocalization of NLSE can be observed by both $A(t)$ and $\mathbb{E}(|\psi^\epsilon_{H,h}|^2)$.

5.3.2. Convergence of MC sampling and qMC sampling. The MC method and qMC method have different convergence rates. Hence we check the numerical convergence rate of the MC method and qMC method. To eliminate the perturbation of a small sample size, we adopt the random potential

$$v(x, \omega) = 1.0 + \sigma \sum_{j=1}^{m} \sin(jx) \frac{1}{j^\beta} \xi_j(\omega), \tag{5.5}$$

in which the parameters are: $\sigma = 1.0$, $\beta = 2.0$, $m = 5$. The other simulation settings are: $\lambda = 0.1$, $\epsilon = \frac{1}{8}$, $\mathcal{D} = [-\pi, \pi]$, $h = \frac{2\pi}{600}$, $H = 6h$, $T = 1.0$ and $\Delta t =$1.0e-03. In this experiment, we use 50000 samples to compute the reference solution and record the

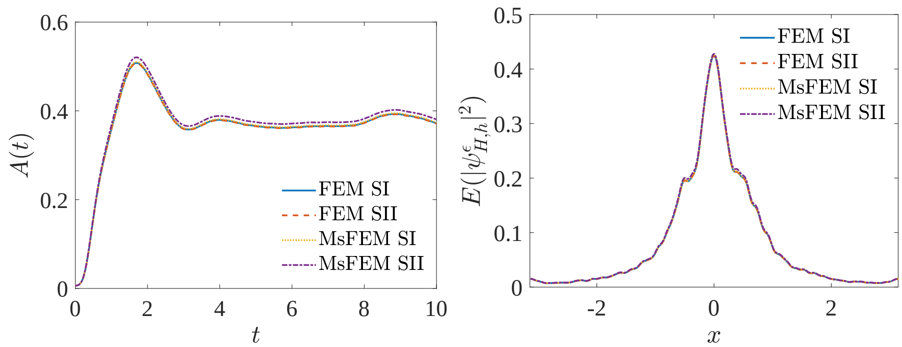

(a) Linear case.

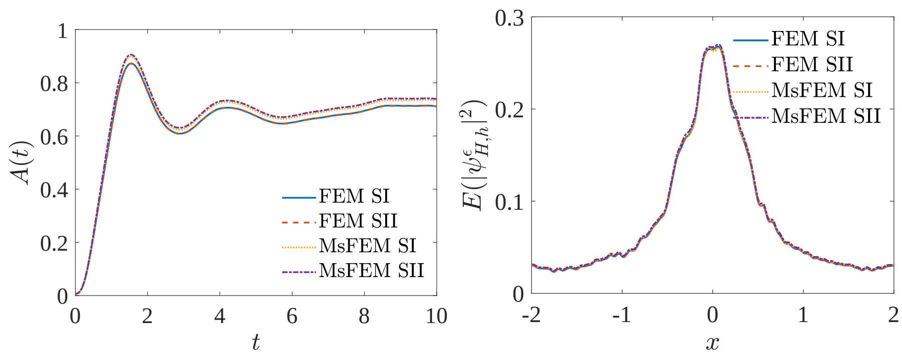

(b) Nonlinear case with $\lambda = 1.0$.

Fig. 5: Numerical results computed by FEM and MsFEM with different time-splitting methods for the NLSE with $\lambda = 0$ and $\lambda = 1.0$.

L^2 error of the density $\|\mathbb{E}(|\psi^{\epsilon}_{\mathrm{num}}|^2) - \mathbb{E}(|\psi^{\epsilon}_{\mathrm{ref}}|^2)\|$ as the sampling number varies with $N = 100$, 200, 400, 800, 1600 and 3200 for both MC method and qMC method. The result is shown in Figure 6.

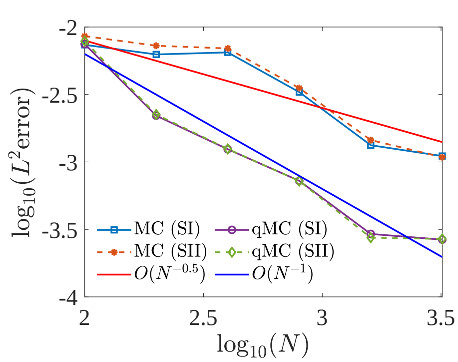

Fig. 6: Numerical convergence rates of the MC and qMC methods.

5.3.3. Investigation of wave propagation. For the 1D case, we vary λ and record the evolution of $A(t)$ to observe the wave propagation phenomena. As well as we depict $\mathbb{E}(|\psi^{\epsilon}_{H,h}|^2)$ at terminal time. Here 500 qMC samples are generated to approximate the random potential. The parameters of simulations are: $\mathcal{D} = [-2\pi, 2\pi]$, $\sigma = 1.0$, $\beta = 0.0$ and $m = 5$. For the MsFEM, we fix $h = \frac{4\pi}{6000}$ and $H = 10h$. To observe the long-time behavior, we set the terminal time to be $T = 20$. We vary the nonlinear coefficient $\lambda = 0, 1, 10, 20$, and the results are shown in Figure 7. $A(t)$ increases as time evolves for nonlinear cases, while it floats within a range of

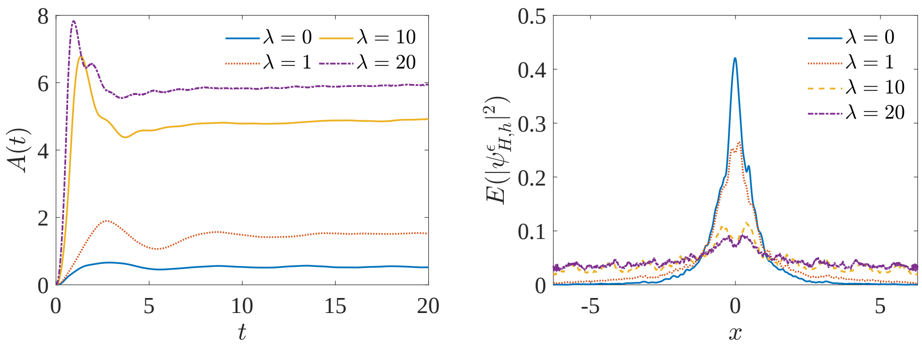

Fig. 7: The evolution of $A(t)$ and density of expectation at $T = 20$, as the nonlinear coefficient λ varies. Results computed by the **SI** and MsFEM.

$(0.51, 0.57)$ for the linear case during the time interval $t = 10$ to $t = 20$.

Next, we consider the 2D equation. The settings in our numerical simulations are: $h = \frac{1}{64}$, $\epsilon = \frac{1}{4}$, $H = 4h$, $\beta = 0$, $m = 5$ and $\sigma = 5$. As shown in Figure 8 and Figure 9, the localization and delocalization of mass distribution are observed for linear and nonlinear cases, respectively.

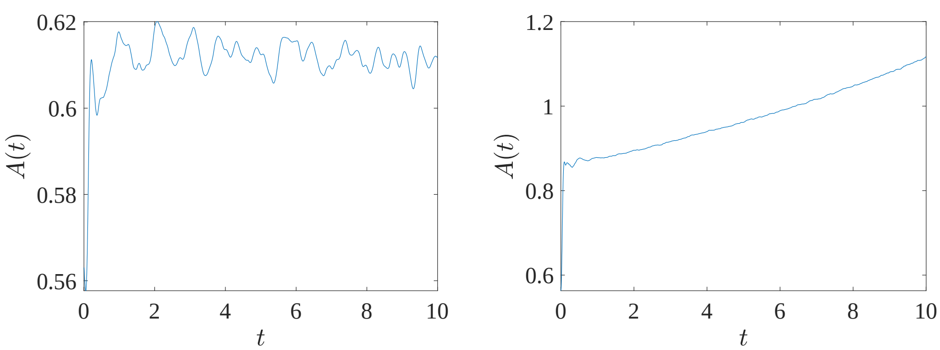

Fig. 8: The evolution of $A(t)$ for 2D linear case and nonlinear case with $\lambda = 20$. Results are computed by **SI** and MsFEM.

6. Conclusion.

In this work, we present two time-splitting finite element methods (TS-FEMs) for the cubic nonlinear Schrödinger equation (NLSE). We introduce

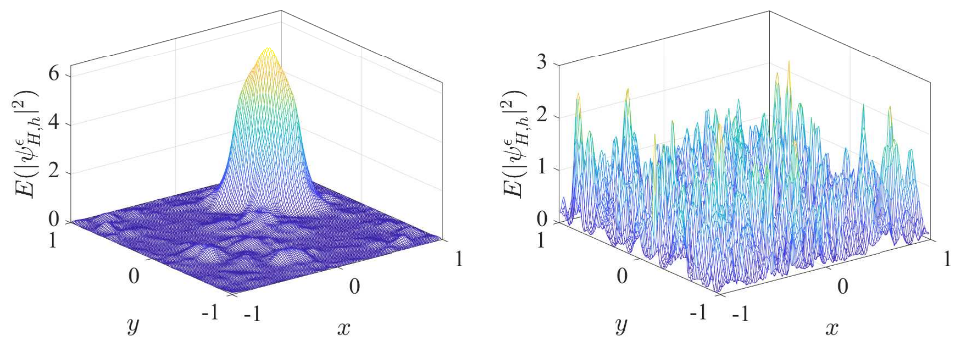

Fig. 9: The localization and delocalization of mass distribution of the 2D linear Schrödinger equation and NLSE with random potentials, respectively.

the multiscale finite element method (MsFEM) to reduce the spatial degrees of freedom. The multiscale basis functions are constructed by solving a set of optimal problems with local orthogonal normalization constraints. We find that a mesh-dependent scale is involved in the basis functions because of the localized orthogonal normalization constraints, which produce an indispensable scale in the numerical solution. We revised the optimal problems to address this issue in this work. For time evolving, we present two Strang time-splitting manners in which one can maintain the convergence rate for the NLSE with discontinuous potentials. Accounting for the random potential, we employ the quasi-Monte Carlo sampling method in the random space. Thus our approaches yield the numerical solution with second-order accuracy in both time and space, and an almost first-order convergence rate in the random space. We provide a theoretical convergence of the L^2 error estimate, corroborating the convergence through numerical experiments. In addition, we present a multiscale reduced basis method that reduces the computational burden of constructing the multiscale basis functions for random potentials. By the proposed methods, the long-time wave propagation of the NLSE with parameterized random potentials in 1D and 2D physical space is investigated efficiently. The localization of the linear case and delocalization of the nonlinear case are observed. In summary, the proposed TS-MsFEMs offer a valuable approach for simulating the NLSE with random potentials, achieving good accuracy and high efficiency.

Declaration of interest. The authors report no conflict of interest.

Appendix A. A multiscale reduced basis method. As a supplement, here we present an approach to reduce the computational effort of construction basis functions for random potentials. This approach is motivated by the method proposed in [15], which consists of offline and online stages. In the offline stage, let $\{v(\boldsymbol{x}, \omega_q)\}_{q=1}^{Q}$ be the samples of potential with Q the number of samples. At the node $\boldsymbol{x}_p$, $\zeta_p^0 = \frac{1}{Q}\sum_{q=1}^{Q} \phi_p(\boldsymbol{x}, \omega_q)$ is the sample mean of basis functions, and $\tilde{\phi}_p(\boldsymbol{x}, \omega_q) = \phi_p(\boldsymbol{x}, \omega_q) - \zeta_p^0$ is the fluctuation. Employ the POD method to $\{\tilde{\phi}_p(\boldsymbol{x}, \omega_q)\}_{q=1}^{Q}$ build a reduced basis functions $\{\zeta_p^1(\boldsymbol{x}), \cdots, \zeta_p^{m_p}(\boldsymbol{x})\}$ with $m_p \ll Q$. In the online stage, the multiscale basis function at $\boldsymbol{x}_p$ has the form

$$\phi_p(\boldsymbol{x},\omega) = \sum_{l=0}^{m_p} c_p^l(\omega)\zeta_p^l(\boldsymbol{x}), \tag{A.1}$$

in which $\{c_p^l\}_{l=0}^{m_p}$ are unknowns. Due to the wave function being represented by

$$\psi_H^\epsilon(\boldsymbol{x},t,\omega) = \sum_{p=1}^{N_H}\sum_{l=0}^{m_p} c_p^l(t,\omega)\zeta_p^l(\boldsymbol{x}), \tag{A.2}$$

the dofs in the Galerkin formulation is $\sum_{p=1}^{N_H}(m_p+1)$. To reduce the dofs of the Galerkin formulation, we compute $\{c_p^l\}_{l=0}^{m_p}$ in (A.1) by solving the following reduced optimal problems

$$\min a(\phi_p,\phi_p), \tag{A.3}$$

$$\text{s.t.} \int_{\mathcal{D}} \phi_p\phi_q^H \mathrm{d}\mathbf{x} = \lambda(H)\delta_{pq}, \quad \forall 1\le q\le N_H. \tag{A.4}$$

Owing to the value of m_p could be small [15], the computation cost of constructing the multiscale basis functions can be saved, and the dofs in the Galerkin formulation is still N_H in the online stage. In addition, we adopt parallel implementations with 12 cores in the following tests.

To substantiate the improvement of the reduced MsFEM basis method, we carry out two numerical tests. We fix $m_p = 3$ for $p = 1,\cdots,N_H$, and generate 1000 samples by the qMC method with 200 samples allocated for the offline stage and the remaining 800 samples used in the online stage. The**SI** is employed for time evolving.

Here the experiment of the nonlinear case in 5.3.1 is conducted. We compare the numerical solution computed by the FEM, MsFEM, and the MsFEM with the POD reduction method as in Figure 10.

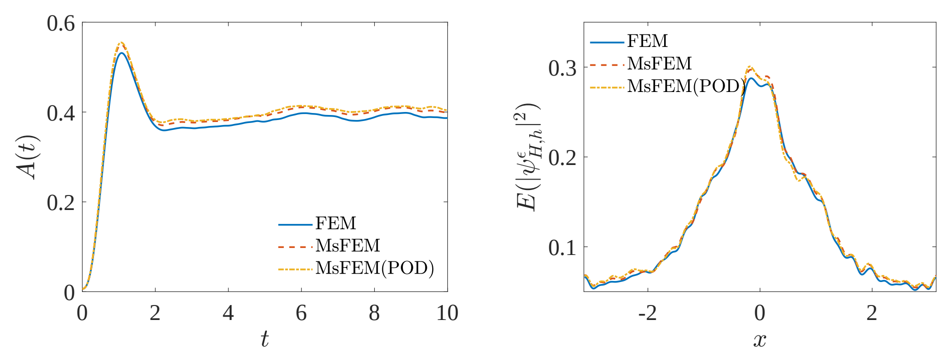

Fig. 10: Numerical comparison of FEM, MsFEM and the MsFEM with POD reduction methods.

Furthermore, we vary the qMC samples and record the corresponding time costs in Table 3. Note that the time costs of MsFEM with the POD reduction are attributed to both the offline and online stages of the computations. As illustrated in Table 3, a considerable enhancement in simulation efficiency is achieved through the application of MsFEM, with additional improvements attained in the integration of the POD reduction method.

Table 3: Comparison of time costs (second) for the FEM, MsFEM, and the MsFEM with POD reduction methods.

Sample number	FEM	MsFEM	MsFEM (POD) (offline)
1000	2116	152	107 (35)
2000	4205	308	243 (35)
4000	8376	620	501 (34)
8000	16633	1239	1020 (40)
16000	33469	2466	2137 (43)

We repeat the experiment of NLSE with $\lambda = 20$ as in 5.3.3. The corresponding numerical results are shown in Figure 11. The MsFEM combined with the POD reduction method takes approximately 14978 seconds (4.16 hours), with 1064 seconds spent on the offline stage. In contrast, the MsFEM without incorporating the POD method takes 20,061 seconds (5.57 hours).

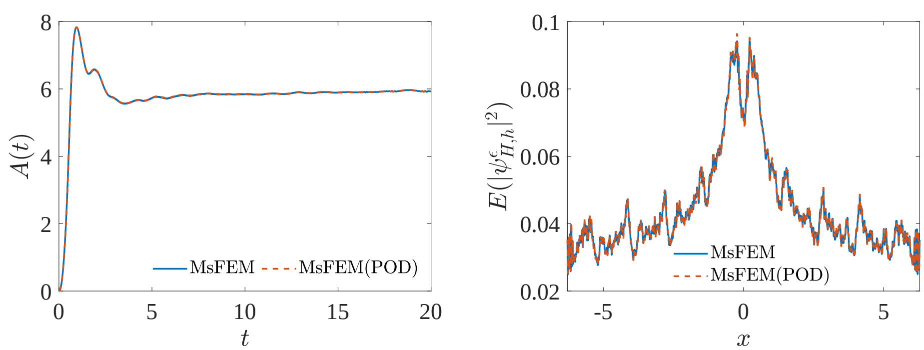

Fig. 11: Numerical comparison of MsFEM method and the MsFEM with the POD reduction method for the 1D NLSE with $\lambda = 20$.

Appendix B. The proof of Lemma 2.1.

Proof. We first study the regularity of ψ^ϵ in space. Since the energy is a constant

$$E(t) = \frac{\epsilon^2}{2}\|\nabla\psi^\epsilon\|^2 + (v, |\psi^\epsilon|^2) + \frac{\lambda}{2}\|\psi^\epsilon\|^4_{L^4} = E_0 < \infty$$

with $\lambda \geq 0$, we directly get

$$\frac{\epsilon^2}{2}\|\nabla\psi^\epsilon\|^2 = E_0 - (v, |\psi^\epsilon|^2) - \frac{\lambda}{2}\|\psi^\epsilon\|^4_{L^4} \leq E_0 + \|v\|_\infty,$$

which means

$$\|\nabla\psi^\epsilon\| \leq \frac{C}{\epsilon}.$$

Meanwhile, we also have

$$\|\psi^\epsilon\|_{L^4}^4 \le \frac{E_0 + \|v\|_\infty}{\lambda}. \tag{B.1}$$

Owing to the Hamiltonian $\mathcal{H}$ is not explicitly dependent on time, and $[\mathcal{H}^2, \mathcal{H}] = 0$, the following average value of mechanics quantity is independent of time, i.e.,

$$(\mathcal{H}^2\psi^\epsilon, \psi^\epsilon) = E_1 \tag{B.2}$$

with $\mathrm{d}_t E_1 = 0$. Explicitly, we have

$$\begin{aligned}(\mathcal{H}^2\psi^\epsilon, \psi^\epsilon) =& \frac{\epsilon^4}{4}(\Delta^2\psi^\epsilon, \psi^\epsilon) + (v^2\psi^\epsilon, \psi^\epsilon) + \lambda^2(|\psi^\epsilon|^4\psi^\epsilon, \psi^\epsilon) \\ &- \epsilon^2(\Delta v\psi^\epsilon, \psi^\epsilon) + 2\lambda(v|\psi^\epsilon|^2\psi^\epsilon, \psi^\epsilon) - \lambda\epsilon^2(\Delta|\psi^\epsilon|^2\psi^\epsilon, \psi^\epsilon).\end{aligned}$$

We then get

$$\begin{aligned}&\frac{\epsilon^4}{4}\|\Delta\psi^\epsilon\|^2 + \|v\psi^\epsilon\|^2 + \lambda^2\|\psi^\epsilon\|_{L^6}^6 \\ \le& E_1 + \epsilon^2(\Delta v\psi^\epsilon, \psi^\epsilon) - 2\lambda(v|\psi^\epsilon|^2\psi^\epsilon, \psi^\epsilon) + \lambda\epsilon^2(\Delta|\psi^\epsilon|^2\psi^\epsilon, \psi^\epsilon) \\ \le& E_1 - \epsilon^2(\nabla v\psi^\epsilon, \nabla\psi^\epsilon) + 2\lambda\|v\|_\infty\|\psi^\epsilon\|_{L^4}^4 + 3\lambda\epsilon^2\|\psi^\epsilon\|_\infty^2\|\nabla\psi^\epsilon\|^2 \\ \le& E_1 + C\|v\|_\infty + \epsilon\|\nabla v\|_\infty + 2\lambda\|v\|_\infty\|\psi^\epsilon\|_{L^4}^4 + 3\lambda C\|\psi^\epsilon\|_\infty^2.\end{aligned}$$

Hence, there exists a constant C that depends on $\|v\|_\infty$, $\|\nabla v\|_\infty$, E_0, E_1, and $\|\psi^\epsilon\|_\infty$ such that

$$\|\nabla^2\psi^\epsilon\| \le \frac{C}{\epsilon^2}, \quad \|\psi^\epsilon\|_{L^6}^6 \le \frac{C}{\lambda^2}. \tag{B.3}$$

Furthermore, if $\psi^\epsilon \in H^4$, we also have $[\mathcal{H}^s, \mathcal{H}] = 0$ for $s \le 4$. Repeat the above procedures and we can get

$$\|\nabla^s\psi^\epsilon\| \le \frac{C}{\epsilon^s}. \tag{B.4}$$

Next, we study the bound of $\|\partial_t\psi^\epsilon\|_{H^s}$ with $0 \le s \le 2$. Taking the time derivative for (2.1) yields

$$i\epsilon\partial_{tt}\psi^\epsilon = -\frac{\epsilon^2}{2}\Delta\partial_t\psi^\epsilon + v\partial_t\psi^\epsilon + 2\lambda|\psi^\epsilon|^2\partial_t\psi^\epsilon + \lambda(\psi^\epsilon)^2\partial_t\bar{\psi}^\epsilon. \tag{B.5}$$

Take inner product of this equation with $\partial_t\psi^\epsilon$ and we get

$$i\epsilon\mathrm{d}_t(\partial_t\psi^\epsilon, \partial_t\psi^\epsilon) = \lambda\int_{\mathcal{D}}(\partial_t\psi^\epsilon\bar{\psi}^\epsilon)^2 - (\partial_t\bar{\psi}^\epsilon\psi^\epsilon)^2\mathrm{d}\boldsymbol{x} = 4i\lambda\int_{\mathcal{D}}\Re(\partial_t\psi^\epsilon\bar{\psi}^\epsilon)\Im(\partial_t\psi^\epsilon\bar{\psi}^\epsilon)\mathrm{d}\boldsymbol{x}. \tag{B.6}$$

Thus we have

$$\epsilon\mathrm{d}_t\|\partial_t\psi^\epsilon\|^2 \le 2\lambda\|\partial_t\psi^\epsilon\psi^\epsilon\|^2 \le 2\lambda\|\psi^\epsilon\|_\infty^2\|\partial_t\psi^\epsilon\|^2,$$

which indicates

$$\|\partial_t\psi^\epsilon\| \le \|\partial_t\psi_{\mathrm{in}}\|\exp\left(\frac{2\lambda T\|\psi^\epsilon\|_\infty^2}{\epsilon}\right). \tag{B.7}$$

For the initial condition, we have

$$\|\partial_t \psi_{\rm in}\| \le \frac{\epsilon}{2}\|\nabla\psi_{\rm in}\| + \frac{1}{\epsilon}(v\psi_{\rm in},\psi_{\rm in}) + \frac{\lambda}{\epsilon}\|\psi_{\rm in}\|_{L^4}^2 \le \frac{C}{\epsilon}.$$

We therefore get

$$\|\partial_t\psi^\epsilon\| \le \frac{C}{\epsilon}\exp\left(\frac{2\lambda\|\psi^\epsilon\|_\infty^2 T}{\epsilon}\right). \tag{B.8}$$

Take inner product of the equation (B.5) with $\partial_t\Delta\psi^\epsilon$, and we have

$$\begin{aligned}\epsilon \mathrm{d}_t\|\nabla\partial_t\psi^\epsilon\|^2 = \Im\{&2(\nabla v\partial_t\psi^\epsilon,\nabla\partial_t\psi^\epsilon) + 4\lambda(\psi^\epsilon\partial_t\psi^\epsilon\nabla\bar{\psi}^\epsilon,\nabla\partial_t\psi^\epsilon)\\ &+4\lambda(\bar{\psi}^\epsilon\partial_t\psi^\epsilon\nabla\psi^\epsilon,\nabla\partial_t\psi^\epsilon) + 4\lambda(\psi^\epsilon\partial_t\psi^\epsilon\nabla\psi^\epsilon,\nabla\partial_t\psi^\epsilon) + 2\lambda((\psi^\epsilon)^2,(\nabla\partial_t\psi^\epsilon)^2)\}.\end{aligned}$$

By the inequalities

$$\begin{aligned}&\|\psi^\epsilon\partial_t\psi^\epsilon\nabla\psi^\epsilon\nabla\partial_t\psi^\epsilon\|_{L^1} \le \|\psi^\epsilon\|_{L^6}\|\partial_t\psi^\epsilon\|_{L^6}\|\nabla\psi^\epsilon\|_{L^6}\|\nabla\partial_t\psi^\epsilon\|\\ \le &C\|\psi^\epsilon\|_{L^6}\left(\frac{d}{3}\|\partial_t\nabla\psi^\epsilon\| + \left(1-\frac{d}{3}\right)\|\partial_t\psi^\epsilon\|\right)\|\nabla^2\psi^\epsilon\|^{\frac12+\frac{d}{6}}\|\nabla\partial_t\psi^\epsilon\|\\ \le &C\|\psi^\epsilon\|_{L^6}\left(\|\partial_t\nabla\psi^\epsilon\| + \|\partial_t\psi^\epsilon\|\right)\|\nabla^2\psi^\epsilon\|\|\nabla\partial_t\psi^\epsilon\|\end{aligned}$$

and

$$\|(\psi^\epsilon)^2(\nabla\partial_t\psi^\epsilon)^2\|_{L^1} \le \|\psi^\epsilon\|_{L^\infty}^2\|\nabla\partial_t\psi^\epsilon\|^2,$$

we get

$$\epsilon \mathrm{d}_t\|\partial_t\nabla\psi^\epsilon\| \le 2\|\nabla v\|_\infty\|\partial_t\psi^\epsilon\| + C\lambda\|\nabla^2\psi^\epsilon\|\left(\|\partial_t\nabla\psi^\epsilon\| + \|\partial_t\psi^\epsilon\|\right) + 2\lambda\|\psi^\epsilon\|_{L^\infty}^2\|\nabla\partial_t\psi^\epsilon\|.$$

Then we arrive at

$$\begin{aligned}\|\partial_t\nabla\psi^\epsilon\| &\le \left(\frac{2\|\nabla v\|_\infty}{\epsilon} + \frac{C\lambda\|\nabla^2\psi^\epsilon\|}{\epsilon}\right)\|\partial_t\psi^\epsilon\|\exp\left(\frac{C\lambda T\|\nabla^2\psi^\epsilon\|}{\epsilon} + \frac{2\lambda T\|\psi^\epsilon\|_\infty^2}{\epsilon}\right)\\ &\le \frac{C\lambda}{\epsilon^4}\exp\left(\frac{C\lambda T}{\epsilon^3}\right).\end{aligned}$$

Let $d=3$, and the above result can be replaced with

$$\|\partial_t\nabla\psi^\epsilon\| \le \frac{2\|\nabla v\|_\infty}{\epsilon}\|\partial_t\psi^\epsilon\|\exp\left(\frac{C\lambda T\|\nabla^2\psi^\epsilon\|}{\epsilon} + \frac{2\lambda T\|\psi^\epsilon\|_\infty^2}{\epsilon}\right). \tag{B.9}$$

By the similar procedures, we have

$$\begin{aligned}\epsilon \mathrm{d}_t\|\partial_t\nabla^2\psi^\epsilon\|^2 \le &\|\nabla^2 v\|_\infty\|\partial_t\psi^\epsilon\|\|\partial_t\nabla^2\psi^\epsilon\| + 2\|\nabla v\|_\infty\|\partial_t\nabla\psi^\epsilon\|\|\partial_t\nabla^2\psi^\epsilon\| +\\ &C\lambda\|\nabla^3\psi^\epsilon\|^{\frac23+\frac{d}{9}}\|\partial_t\nabla\psi^\epsilon\|^{\frac{d}{3}}\|\partial_t\psi^\epsilon\|^{1-\frac{d}{3}}\|\partial_t\nabla^2\psi^\epsilon\| +\\ &C\lambda\|\nabla^3\psi^\epsilon\|^{\frac{6}{9-d}}\|\psi^\epsilon\|_{L^6}^{2-\frac{6}{9-d}}\|\partial_t\nabla\psi^\epsilon\|^{\frac{d}{3}}\|\partial_t\psi^\epsilon\|^{1-\frac{d}{3}}\|\partial_t\nabla^2\psi^\epsilon\| +\\ &C\lambda\|\nabla^2\psi^\epsilon\|^{\frac12+\frac{d}{6}}\|\partial_t\nabla^2\psi^\epsilon\|^{\frac12+\frac{d}{6}}\|\partial_t\psi^\epsilon\|^{\frac12-\frac{d}{6}}\|\partial_t\nabla^2\psi^\epsilon\| + C\lambda\|\psi^\epsilon\|_\infty^2\|\partial_t\nabla^2\psi^\epsilon\|^2\end{aligned}$$

in which we use the inequalities

$$
\begin{aligned}
\|\nabla^2\psi^\epsilon\psi^\epsilon\partial_t\psi^\epsilon\partial_t\nabla^2\psi^\epsilon\|_{L^1} &\le \|\psi^\epsilon\|_{L^6}\|\nabla^2\psi^\epsilon\|_{L^6}\|\partial_t\psi^\epsilon\|_{L^6}\|\partial_t\nabla^2\psi^\epsilon\| \\
&\le C\|\nabla^3\psi^\epsilon\|^{\frac{2}{3}+\frac{d}{9}}\|\partial_t\nabla\psi^\epsilon\|^{\frac{d}{3}}\|\partial_t\psi^\epsilon\|^{1-\frac{d}{3}}\|\partial_t\nabla^2\psi^\epsilon\|, \\
\|\nabla\psi^\epsilon\nabla\psi^\epsilon\partial_t\psi^\epsilon\partial_t\nabla^2\psi^\epsilon\|_{L^1} &\le \|\nabla\psi^\epsilon\|_{L^6}^2\|\partial_t\psi^\epsilon\|_{L^6}\|\partial_t\nabla^2\psi^\epsilon\| \\
&\le C\|\nabla^3\psi^\epsilon\|^{\frac{6}{9-d}}\|\psi^\epsilon\|_{L^6}^{2-\frac{6}{9-d}}\|\partial_t\nabla\psi^\epsilon\|^{\frac{d}{3}}\|\partial_t\psi^\epsilon\|^{1-\frac{d}{3}}\|\partial_t\nabla^2\psi^\epsilon\|, \\
\|\psi^\epsilon\nabla\psi^\epsilon\partial_t\nabla\psi^\epsilon\partial_t\nabla^2\psi^\epsilon\|_{L^1} &\le \|\psi^\epsilon\|_{L^6}\|\nabla\psi^\epsilon\|_{L^6}\|\partial_t\nabla\psi^\epsilon\|_{L^6}\|\partial_t\nabla^2\psi^\epsilon\| \\
&\le C\|\nabla^2\psi^\epsilon\|^{\frac{1}{2}+\frac{d}{6}}\|\partial_t\nabla^2\psi^\epsilon\|^{\frac{1}{2}+\frac{d}{6}}\|\partial_t\psi^\epsilon\|^{\frac{1}{2}-\frac{d}{6}}\|\partial_t\nabla^2\psi^\epsilon\|,
\end{aligned}
$$

and

$$\|(\psi^\epsilon)^2(\partial_t\nabla^2\psi^\epsilon)\|_{L^1} \le \|\psi^\epsilon\|_\infty^2\|\partial_t\nabla^2\psi^\epsilon\|^2.$$

Then we get

$$\|\partial_t\nabla^2\psi^\epsilon\| \le \frac{C\lambda\|\nabla^3\psi^\epsilon\|^\ell\|\partial_t\nabla\psi^\epsilon\|^{\frac{d}{3}}\|\partial_t\psi^\epsilon\|^{1-\frac{d}{3}}}{\epsilon}\exp\left(\frac{C\lambda T\|\nabla^2\psi^\epsilon\| + C\lambda T\|\psi^\epsilon\|_\infty^2}{\epsilon}\right), \tag{B.10}$$

where $\ell = \max\{\frac{2}{3}+\frac{d}{9}, \frac{6}{9-d}\}$. Let $d=3$ and we get the compact form

$$\|\partial_t\nabla^2\psi^\epsilon\| \le \frac{C\lambda\|\nabla^3\psi^\epsilon\|}{\epsilon}\|\partial_t\nabla\psi^\epsilon\|\exp\left(\frac{C\lambda T\|\nabla^2\psi^\epsilon\| + C\lambda T\|\psi^\epsilon\|_\infty^2}{\epsilon}\right). \tag{B.11}$$

Due to $\epsilon \ll 1$, the order of $\|\partial_t\psi^\epsilon\|_{H^s}$ with respect to ϵ directly depends on the estimate $\|\partial_t\nabla^s\psi^\epsilon\|$. Thus, there exists a constant $C_{\lambda,\epsilon}$ that depends on λ and ϵ such that $\|\partial_t\psi^\epsilon\|_{H^s} \le C_{\lambda,\epsilon}$. This completes the proof. ∎

Appendix C. The proof of Lemma 4.8.

Proof. Let $|\boldsymbol{\nu}| = 1$, and we take the derivative with respect to $\xi_j(\omega)$ of (2.10). Denote $\partial_j\psi_m = \partial_{\xi_j}\psi_m^\epsilon$ and $\partial_j v_m = \partial_{\xi_j}v_m^\epsilon$, and we get

$$i\epsilon\partial_t(\partial_j\psi_m) = -\frac{\epsilon^2}{2}\Delta(\partial_j\psi_m) + (\partial_j v_m)\psi_m^\epsilon + v_m^\epsilon(\partial_j\psi_m) + \lambda(2|\psi_m^\epsilon|^2\partial_j\psi_m + (\psi_m^\epsilon)^2\partial_j\bar{\psi}_m).$$

We have

$$
\begin{aligned}
&\epsilon \mathrm{d}_t\|\partial_j\psi_m\| \le 2\|\partial_j v_m\|_\infty + 2\lambda\|\psi_m^\epsilon\|_\infty^2\|\partial_j\psi_m\|, \\
&\epsilon \mathrm{d}_t\|\nabla\partial_j\psi_m\| \le 2\|\nabla\partial_j v_m\|_\infty + 2\|\partial_j v_m\|_\infty\|\nabla\psi_m^\epsilon\| + 2\|\nabla v_m\|_\infty\|\partial_j\psi_m\| + \\
&\quad 16\lambda\|\psi_m^\epsilon\|_\infty\|\partial_j\psi_m\|_{L^4}\|\nabla\psi_m^\epsilon\|_{L^4} + 2\lambda\|\psi_m^\epsilon\|_\infty^2\|\nabla\partial_j\psi_m\|, \\
&\epsilon \mathrm{d}_t\|\nabla^2\partial_j\psi_m\| \le 2\|\nabla^2\partial_j v_m\|_\infty + 4\|\nabla\partial_j v_m\|_\infty\|\nabla\psi_m^\epsilon\| + 2\|\partial_j v_m\|_\infty\|\nabla^2\psi_m^\epsilon\| + \\
&\quad 2\|\nabla^2 v_m\|_\infty\|\partial_j\psi_m\| + 4\|\nabla v_m\|_\infty\|\nabla\partial_j\psi_m\| + 8\lambda\|\psi_m^\epsilon\|_\infty\|\nabla^2\psi_m^\epsilon\|_{L^4}\|\partial_j\psi_m\|_{L^4} + \\
&\quad 8\lambda\|\nabla\psi_m^\epsilon\|_{L^6}^2\|\partial_j\psi_m\|_{L^6} + 16\lambda\|\psi_m^\epsilon\|_\infty\|\nabla\psi_m^\epsilon\|_{L^4}\|\nabla\partial_j\psi_m^\epsilon\|_{L^4} + 2\lambda\|\psi_m^\epsilon\|_\infty^2\|\nabla^2\partial_j\psi_m\|.
\end{aligned}
$$

Owing to

$$\begin{aligned}
\|\partial_j\psi_m\|_{L^4}\|\nabla\psi_m^\epsilon\|_{L^4} &\le C\|\nabla\partial_j\psi_m\|^{\frac{d}{4}}\|\partial_j\psi_m\|^{1-\frac{d}{4}}\|\psi_m\|_{H^2}^{\frac{1}{2}}\|\psi_m\|_\infty^{\frac{1}{2}}\\
&\le C\|\psi_m\|_{H^2}^{\frac{1}{2}}\|\psi_m\|_\infty^{\frac{1}{2}}\left(\frac{d}{4}\|\nabla\partial_j\psi_m\|+\left(1-\frac{d}{4}\right)\|\partial_j\psi_m\|\right),\\
\|\nabla^2\psi_m^\epsilon\|_{L^4}\|\partial_j\psi_m\|_{L^4} &\le C\|\nabla^3\psi_m\|^{\frac{8+d}{12}}\|\psi_m\|^{\frac{4-d}{12}}\left(\frac{d}{4}\|\nabla\partial_j\psi_m\|+\left(1-\frac{d}{4}\right)\|\partial_j\psi_m\|\right),\\
\|\nabla\psi_m^\epsilon\|_{L^6}^2\|\partial_j\psi_m\|_{L^6} &\le C\|\nabla^2\psi_m^\epsilon\|^{1+\frac{d}{3}}\|\psi^\epsilon\|^{1-\frac{d}{3}}\|\nabla\partial_j\psi_m\|^{\frac{d}{3}}\|\partial_j\psi_m\|^{1-\frac{d}{3}}\\
&\le C\|\nabla^2\psi_m^\epsilon\|^{1+\frac{d}{3}}\|\psi^\epsilon\|^{1-\frac{d}{3}}\left(\frac{d}{3}\|\nabla\partial_j\psi_m\|+\left(1-\frac{d}{3}\right)\|\partial_j\psi_m\|\right),
\end{aligned}$$

and

$$\begin{aligned}
\|\nabla\psi_m^\epsilon\|_{L^4}\|\nabla\partial_j\psi_m^\epsilon\|_{L^4} &\le C\|\psi_m\|_{H^2}^{\frac{1}{2}}\|\psi_m\|_\infty^{\frac{1}{2}}\|\nabla^2\partial_j\psi_m\|^{\frac{1}{2}+\frac{d}{8}}\|\partial_j\psi_m\|^{\frac{1}{2}-\frac{d}{8}}\\
&\le C\|\psi_m\|_{H^2}^{\frac{1}{2}}\|\psi_m\|_\infty^{\frac{1}{2}}\left(\left(\frac{1}{2}+\frac{d}{8}\right)\|\nabla^2\partial_j\psi_m\|+\left(\frac{1}{2}-\frac{d}{8}\right)\|\partial_j\psi_m\|\right).
\end{aligned}$$

We can construct

$$\epsilon \mathrm{d}_t\|\partial_j\psi_m\|_{H^2}\le\frac{C_1}{\epsilon^2}\|\partial_j v_m\|_{H^2}+\frac{C_2}{\epsilon^4}\|\partial_j\psi_m\|_{H^2}.$$

Then we get for all $t\in(0,T]$

$$\|\partial_j\psi_m\|_{H^2}\le\frac{C_1 t}{\epsilon^3}\|\partial_j v_m\|_{H^2}\exp\left(\frac{C_2 t}{\epsilon^4}\right)\le C(t,\lambda,\epsilon,|\boldsymbol{\nu}|)\sqrt{\lambda_j}\|v_j\|_{H^2},$$

where $C(t,\lambda,\epsilon,|\boldsymbol{\nu}|)$ depends on t,λ,ϵ but is independent of dimensions.

Then for $|\boldsymbol{\nu}|\ge 2$, by the Leibniz rule we have

$$\begin{aligned}
i\epsilon\partial_t\partial^{\boldsymbol{\nu}}\psi_m^\epsilon &= -\frac{\epsilon^2}{2}\Delta(\partial^{\boldsymbol{\nu}}\psi_m^\epsilon)+\sum_{\boldsymbol{\mu}\preceq\boldsymbol{\nu}}\binom{\boldsymbol{\nu}}{\boldsymbol{\mu}}\partial^{\boldsymbol{\nu}-\boldsymbol{\mu}}v_m\partial^{\boldsymbol{\mu}}\psi_m^\epsilon+\lambda\sum_{\boldsymbol{\mu}\preceq\boldsymbol{\nu}}\binom{\boldsymbol{\nu}}{\boldsymbol{\mu}}\partial^{\boldsymbol{\nu}-\boldsymbol{\mu}}|\psi_m^\epsilon|^2\partial^{\boldsymbol{\mu}}\psi_m^\epsilon\\
&= -\frac{\epsilon^2}{2}\Delta(\partial^{\boldsymbol{\nu}}\psi_m^\epsilon)+v_m\partial^{\boldsymbol{\nu}}\psi_m^\epsilon+\lambda(2|\psi_m^\epsilon|^2\partial^{\boldsymbol{\nu}}\psi_m^\epsilon+(\psi_m^\epsilon)^2\partial^{\boldsymbol{\nu}}\bar\psi_m^\epsilon)+\\
&\sum_{\substack{\boldsymbol{\mu}\prec\boldsymbol{\nu},\\ |\boldsymbol{\nu}-\boldsymbol{\mu}|=1}}\binom{\boldsymbol{\nu}}{\boldsymbol{\mu}}\partial^{\boldsymbol{\nu}-\boldsymbol{\mu}}v_m\partial^{\boldsymbol{\mu}}\psi_m^\epsilon+\lambda\sum_{\boldsymbol{\mu}\prec\boldsymbol{\nu}}\binom{\boldsymbol{\nu}}{\boldsymbol{\mu}}\sum_{\boldsymbol{\eta}\preceq\boldsymbol{\nu}-\boldsymbol{\mu}}\binom{\boldsymbol{\nu}-\boldsymbol{\mu}}{\boldsymbol{\eta}}\partial^{\boldsymbol{\nu}-\boldsymbol{\mu}-\boldsymbol{\eta}}\psi_m^\epsilon\partial^{\boldsymbol{\mu}}\bar\psi_m^\epsilon\partial^{\boldsymbol{\eta}}\psi_m^\epsilon.
\end{aligned}$$

Repeat the above procedures, and we get

$$\epsilon \mathrm{d}_t \|\partial^{\boldsymbol{\nu}} \psi_m^\epsilon\| \le 2|\boldsymbol{\nu}| \sum_{|\boldsymbol{\nu}-\boldsymbol{\mu}|=1} \|\partial^{\boldsymbol{\nu}-\boldsymbol{\mu}} v_m\|_\infty \|\partial^{\boldsymbol{\mu}} \psi_m^\epsilon\| + 2\lambda \|\psi^\epsilon\|_\infty^2 \|\partial^{\boldsymbol{\nu}} \psi_m^\epsilon\| +$$

$$2\lambda \sum_{\boldsymbol{\mu}\prec\boldsymbol{\nu}} \binom{\boldsymbol{\nu}}{\boldsymbol{\mu}} \sum_{\boldsymbol{\eta}\preceq\boldsymbol{\nu}-\boldsymbol{\mu}} \binom{\boldsymbol{\nu}-\boldsymbol{\mu}}{\boldsymbol{\eta}} \|\partial^{\boldsymbol{\nu}-\boldsymbol{\mu}-\boldsymbol{\eta}} \psi_m^\epsilon\|_{L^6} \|\partial^{\boldsymbol{\mu}} \psi_m^\epsilon\|_{L^6} \|\partial^{\boldsymbol{\eta}} \psi_m^\epsilon\|_{L^6},$$

$$\epsilon \mathrm{d}_t \|\nabla \partial^{\boldsymbol{\nu}} \psi_m^\epsilon\| \le 2\|\nabla v_m\|_\infty \|\partial^{\boldsymbol{\nu}} \psi_m\| + 2\lambda C(\|\nabla \psi_m^\epsilon\|_{L^4} \|\partial^{\boldsymbol{\nu}} \psi_m^\epsilon\|_{L^4} + \|\nabla \partial^{\boldsymbol{\nu}} \psi_m^\epsilon\|)$$

$$+ 2|\boldsymbol{\nu}| \sum_{|\boldsymbol{\nu}-\boldsymbol{\mu}|=1} (\|\nabla \partial^{\boldsymbol{\nu}-\boldsymbol{\mu}} v_m\|_\infty \|\partial^{\boldsymbol{\mu}} \psi_m^\epsilon\| + \|\partial^{\boldsymbol{\nu}-\boldsymbol{\mu}} v_m\|_\infty \|\nabla \partial^{\boldsymbol{\mu}} \psi_m^\epsilon\|) +$$

$$2\lambda \sum_{\boldsymbol{\mu}\prec\boldsymbol{\nu}} \binom{\boldsymbol{\nu}}{\boldsymbol{\mu}} \sum_{\boldsymbol{\eta}\preceq\boldsymbol{\nu}-\boldsymbol{\mu}} \binom{\boldsymbol{\nu}-\boldsymbol{\mu}}{\boldsymbol{\eta}} \Big[\|\nabla \partial^{\boldsymbol{\nu}-\boldsymbol{\mu}-\boldsymbol{\eta}} \psi_m^\epsilon\|_{L^6} \|\partial^{\boldsymbol{\mu}} \psi_m^\epsilon\|_{L^6} \|\partial^{\boldsymbol{\eta}} \psi_m^\epsilon\|_{L^6} +$$

$$\|\partial^{\boldsymbol{\nu}-\boldsymbol{\mu}-\boldsymbol{\eta}} \psi_m^\epsilon\|_{L^6} \|\nabla \partial^{\boldsymbol{\mu}} \psi_m^\epsilon\|_{L^6} \|\partial^{\boldsymbol{\eta}} \psi_m^\epsilon\|_{L^6} + \|\partial^{\boldsymbol{\nu}-\boldsymbol{\mu}-\boldsymbol{\eta}} \psi_m^\epsilon\|_{L^6} \|\partial^{\boldsymbol{\mu}} \psi_m^\epsilon\|_{L^6} \|\nabla \partial^{\boldsymbol{\eta}} \psi_m^\epsilon\|_{L^6} \Big].$$

and

$$\epsilon \mathrm{d}_t \|\nabla^2 \partial^{\boldsymbol{\nu}} \psi_m^\epsilon\| \le 2(\|\nabla^2 v_m\|_\infty \|\partial^{\boldsymbol{\nu}} \psi_m\| + \|\nabla v_m\|_\infty \|\nabla \partial^{\boldsymbol{\nu}} \psi_m\|) + 8\lambda \|\nabla \psi_m^\epsilon\|_{L^6}^2 \|\partial^{\boldsymbol{\nu}} \psi_m\|_{L^6}$$

$$+ 8\lambda \|\psi_m^\epsilon\|_\infty \|\nabla^2 \psi_m^\epsilon\|_{L^4} \|\partial^{\boldsymbol{\nu}} \psi_m\|_{L^4} + 16\lambda \|\psi_m^\epsilon\|_\infty \|\nabla \psi_m^\epsilon\|_{L^4} \|\nabla \partial^{\boldsymbol{\nu}} \psi_m^\epsilon\|_{L^4} +$$

$$2|\boldsymbol{\nu}| \sum_{|\boldsymbol{\nu}-\boldsymbol{\mu}|=1} \Big[\|\nabla^2 \partial^{\boldsymbol{\nu}-\boldsymbol{\mu}} v_m\|_\infty \|\partial^{\boldsymbol{\mu}} \psi_m^\epsilon\| + 2\|\nabla \partial^{\boldsymbol{\nu}-\boldsymbol{\mu}} v_m\|_\infty \|\nabla \partial^{\boldsymbol{\mu}} \psi_m^\epsilon\| +$$

$$\|\partial^{\boldsymbol{\nu}-\boldsymbol{\mu}} v_m\|_\infty \|\nabla^2 \partial^{\boldsymbol{\mu}} \psi_m^\epsilon\| \Big] + 2\lambda \|\psi_m^\epsilon\|_\infty^2 \|\nabla^2 \partial^{\boldsymbol{\nu}} \psi_m\| +$$

$$6\lambda C \sum_{\boldsymbol{\mu}\prec\boldsymbol{\nu}} \binom{\boldsymbol{\nu}}{\boldsymbol{\mu}} \sum_{\boldsymbol{\eta}\preceq\boldsymbol{\nu}-\boldsymbol{\mu}} \binom{\boldsymbol{\nu}-\boldsymbol{\mu}}{\boldsymbol{\eta}} \|\partial^{\boldsymbol{\nu}-\boldsymbol{\mu}-\boldsymbol{\eta}} \psi_m^\epsilon\|_{H^2} \|\partial^{\boldsymbol{\mu}} \psi_m^\epsilon\|_{H^2} \|\partial^{\boldsymbol{\eta}} \psi_m^\epsilon\|_{H^2},$$

in which we use the inequality generalized from Proposition 3.6 in [49] as

$$\|\nabla^2 fgh\| \le C\|f\|_{H^2} \|g\|_{H^2} \|h\|_{H^2},$$
$$\|(\nabla f)(\nabla g)h\| \le C\|f\|_{H^2} \|g\|_{H^2} \|h\|_{H^2}.$$

Thus we get

$$\epsilon \mathrm{d}_t \|\partial^{\boldsymbol{\nu}} \psi_m^\epsilon\|_{H^2} \le C_3 \|\partial^{\boldsymbol{\nu}} \psi_m^\epsilon\|_{H^2} + C_4 |\boldsymbol{\nu}| \sum_{|\boldsymbol{\nu}-\boldsymbol{\mu}|=1} \|\partial^{\boldsymbol{\nu}-\boldsymbol{\mu}} v_m\|_{H^2} \|\partial^{\boldsymbol{\mu}} \psi_m^\epsilon\|_{H^2} +$$

$$\lambda C_5 \sum_{\boldsymbol{\mu}\prec\boldsymbol{\nu}} \binom{\boldsymbol{\nu}}{\boldsymbol{\mu}} \sum_{\boldsymbol{\eta}\preceq\boldsymbol{\nu}-\boldsymbol{\mu}} \binom{\boldsymbol{\nu}-\boldsymbol{\mu}}{\boldsymbol{\eta}} \|\partial^{\boldsymbol{\nu}-\boldsymbol{\mu}-\boldsymbol{\eta}} \psi_m^\epsilon\|_{H^2} \|\partial^{\boldsymbol{\mu}} \psi_m^\epsilon\|_{H^2} \|\partial^{\boldsymbol{\eta}} \psi_m^\epsilon\|_{H^2}.$$

An application of the Gronwall inequality yields

$$\|\partial^{\boldsymbol{\nu}} \psi_m^\epsilon\|_{H^2} \le \exp\left(\frac{C_3 T}{\epsilon}\right) \Big\{ \frac{C_4 T |\boldsymbol{\nu}|}{\epsilon} \sum_{|\boldsymbol{\nu}-\boldsymbol{\mu}|=1} \|\partial^{\boldsymbol{\nu}-\boldsymbol{\mu}} v_m\|_{H^2} \|\partial^{\boldsymbol{\mu}} \psi_m^\epsilon\|_{H^2} +$$

$$\frac{\lambda C_5 T}{\epsilon} \sum_{\boldsymbol{\mu}\prec\boldsymbol{\nu}} \binom{\boldsymbol{\nu}}{\boldsymbol{\mu}} \sum_{\boldsymbol{\eta}\preceq\boldsymbol{\nu}-\boldsymbol{\mu}} \binom{\boldsymbol{\nu}-\boldsymbol{\mu}}{\boldsymbol{\eta}} \|\partial^{\boldsymbol{\nu}-\boldsymbol{\mu}-\boldsymbol{\eta}} \psi_m^\epsilon\|_{H^2} \|\partial^{\boldsymbol{\mu}} \psi_m^\epsilon\|_{H^2} \|\partial^{\boldsymbol{\eta}} \psi_m^\epsilon\|_{H^2} \Big\}.$$

Use the induction argument and we get □

$$\|\partial^{\boldsymbol{\nu}} \psi_m\|_{H^2} \le C(t, \lambda, \epsilon, |\boldsymbol{\nu}|) \prod_j (\sqrt{\lambda_j} \|v_j\|_{H^2})^{\nu_j}.$$

REFERENCES

[1] A. Abdulle, W. E, B. Engquist, and E. Vanden-Eijnden, *The heterogeneous multiscale method*, Acta Numer., 21 (2012), p. 1–87.

[2] G. D. Akrivis, V. A. Dougalis, and O. A. Karakashian, *On fully discrete Galerkin methods of second-order temporal accuracy for the nonlinear Schrödinger equation*, Numer. Math., 59 (1991), pp. 31–53.

[3] R. Altmann, P. Henning, and D. Peterseim, *Numerical homogenization beyond scale separation*, Acta Numer., 30 (2021), p. 1–86.

[4] X. Antoine, W. Bao, and C. Besse, *Computational methods for the dynamics of the nonlinear Schrödinger/Gross-Pitaevskii equations*, Comput. Phys. Comm., 184 (2013), pp. 2621–2633.

[5] W. Auzinger, T. Kassebacher, O. Koch, and M. Thalhammer, *Convergence of a Strang splitting finite element discretization for the Schrödinger-Poisson equation*, ESAIM: M2AN, 51 (2017), pp. 1245–1278.

[6] W. Bao and Y. Cai, *Mathematical theory and numerical methods for Bose-Einstein condensation*, Kinet. Relat. Models, 6 (2013), pp. 1–135.

[7] W. Bao, D. Jaksch, and P. A. Markowich, *Numerical solution of the Gross-Pitaevskii equation for Bose-Einstein condensation*, J. Comput. Phys., 187 (2003), pp. 318–342.

[8] W. Bao, S. Jin, and P. A. Markowich, *On time-splitting spectral approximations for the Schrödinger equation in the semiclassical regime*, J. Comput. Phys., 175 (2002), pp. 487–524.

[9] W. Bao, S. Jin, and P. A. Markowich, *Numerical study of time-splitting spectral discretizations of nonlinear Schrödinger equations in the semiclassical regimes*, SIAM J. Sci. Comput., 25 (2003), pp. 27–64.

[10] C. Besse, *A relaxation scheme for the nonlinear schrödinger equation*, SIAM J. Numer. Anal., 42 (2004), pp. 934–952.

[11] C. Besse, B. Bidégaray, and S. Descombes, *Order estimates in time of splitting methods for the nonlinear Schrödinger equation*, SIAM J. Numer. Anal., 40 (2003), pp. 26–40.

[12] C. Besse, S. Descombes, G. Dujardin, and I. Lacroix-Violet, *Energy-preserving methods for nonlinear Schrödinger equations*, IMA J. Numer. Anal., 41 (2020), pp. 618–653.

[13] J. Chen, S. Li, and Z. Zhang, *Efficient multiscale methods for the semiclassical Schrödinger equation with time-dependent potentials*, Comput. Methods Appl. Mech. Engrg., 369 (2020), p. 113232.

[14] J. Chen, D. Ma, and Z. Zhang, *A multiscale finite element method for the Schrödinger equation with multiscale potentials*, SIAM J. Sci. Comput., 41 (2019), pp. B1115–B1136.

[15] J. Chen, D. Ma, and Z. Zhang, *A multiscale reduced basis method for the Schrödinger equation with multiscale and random potentials*, Multiscale Model. Simul., 18 (2020), pp. 1409–1434.

[16] E. T. Chung, Y. Efendiev, and G. Li, *An adaptive GMsFEM for high-contrast flow problems*, J. Comput. Phys., 273 (2014), pp. 54–76.

[17] S. Descombes, *Convergence of a splitting method of high order for reaction-diffusion systems*, Math. Comput., 70 (2001), pp. 1481–1501.

[18] J. Dick, F. Y. Kuo, and I. H. Sloan, *High-dimensional integration: The quasi-Monte Carlo way*, Acta Numer., 22 (2013), p. 133–288.

[19] C. Döding, P. Henning, and J. Wärnegård, *An efficient two level approach for simulating Bose-Einstein condensates*, arXiv preprint arXiv:2212.07392, (2022).

[20] S. Donsa, H. Hofstätter, O. Koch, J. Burgdörfer, and I. Březinová, *Long-time expansion of a Bose-Einstein condensate: Observability of Anderson localization*, Phys. Rev. A, 96 (2017), p. 043630.

[21] W. E and B. Engquist, *The heterognous multiscale methods*, Commun. Math. Sci., 1 (2003), pp. 87–132.

[22] Y. Efendiev, J. Galvis, and T. Y. Hou, *Generalized multiscale finite element methods (GMsFEM)*, J. Comput. Phys., 251 (2013), pp. 116–135.

[23] Y. Efendiev and T. Y. Hou, *Multiscale finite element methods: theory and applications*, vol. 4, Springer Science & Business Media, 2009.

[24] S. Fishman, Y. Krivolapov, and A. Soffer, *The nonlinear Schrödinger equation with a random potential: results and puzzles*, Nonlinearity, 25 (2012), p. R53.

[25] I. García-Mata and D. L. Shepelyansky, *Delocalization induced by nonlinearity in systems with disorder*, Phys. Rev. E, 79 (2009), p. 026205.

[26] I. G. Graham, F. Y. Kuo, J. A. Nichols, R. Scheichl, C. Schwab, and I. H. Sloan, *Quasi-Monte Carlo finite element methods for elliptic PDEs with lognormal random coefficients*, Numer. Math., 131 (2015), pp. 329–368.

[27] P. Henning, A. Målqvist, and D. Peterseim, *Two-level discretization techniques for ground state computations of Bose-Einstein condensates*, SIAM J. Numer. Anal., 52 (2014), pp. 1525–1550.

[28] P. Henning and A. Målqvist, *Localized orthogonal decomposition techniques for boundary value problems*, SIAM J. Sci. Comput., 36 (2014), pp. A1609–A1634.

[29] P. Henning and J. Wärnegård, *Numerical comparison of mass-conservative schemes for the Gross-Pitaevskii equation*, Kinet. Relat. Models, 12 (2019), pp. 1247–1271.

[30] T. Y. Hou, D. Ma, and Z. Zhang, *A model reduction method for multiscale elliptic PDEs with random coefficients using an optimization approach*, Multiscale Model. Simul., 17 (2019), pp. 826–853.

[31] T. Y. Hou and X.-H. Wu, *A multiscale finite element method for elliptic problems in composite materials and porous media*, J. Comput. Phys., 134 (1997), pp. 169–189.

[32] T. Y. Hou and P. Zhang, *Sparse operator compression of higher-order elliptic operators with rough coefficients*, Res. Math. Sci., 4 (2017), p. 24.

[33] A. Iomin, *Subdiffusion in the nonlinear Schrödinger equation with disorder*, Phys. Rev. E, 81 (2010), p. 017601.

[34] K. Karhunen, *Über lineare Methoden in der Wahrscheinlichkeitsrechnung*, Annales Academiae Scientiarum Fennicae: Ser. A 1, Kirjapaino oy. sana, 1947.

[35] M. Knöller, A. Ostermann, and K. Schratz, *A Fourier integrator for the cubic nonlinear Schrödinger equation with rough initial data*, SIAM J. Numer. Anal., 57 (2019), pp. 1967–1986.

[36] S. Li and Z. Zhang, *Computing eigenvalues and eigenfunctions of Schrödinger equations using a model reduction approach*, Commun. Comput. Phys., 24 (2018), pp. 1073–1100.

[37] M. Loeve, *Probability Theory II*, F.W.Gehring P.r.Halmos and C.c.Moore, Springer, 1978.

[38] J. C. López-Marcos and J. M. Sanz-Serna, *A definition of stability for nonlinear problems*, Numerical Treatment of Differential Equations, 104 (1988), pp. 216–226.

[39] A. Målqvist and D. Peterseim, *Computation of eigenvalues by numerical upscaling*, Numer. Math., 130 (2015), pp. 337–361.

[40] A. V. Milovanov and A. Iomin, *Destruction of Anderson localization in quantum nonlinear Schrödinger lattices*, Phys. Rev. E, 95 (2017), p. 042142.

[41] A. Ostermann, Y. Wu, and F. Yao, *A second-order low-regularity integrator for the nonlinear Schrödinger equation*, Adv. Contin. Discrete Models, 2022 (2022), pp. 1–14.

[42] H. Owhadi, *Multigrid with rough coefficients and multiresolution operator decomposition from hierarchical information games*, SIAM Rev., 59 (2017), pp. 99–149.

[43] H. Owhadi and L. Zhang, *Localized bases for finite-dimensional homogenization approximations with nonseparated scales and high contrast*, Multiscale Model. Simul., 9 (2011), pp. 1373–1398.

[44] D. Peterseim, *Eliminating the pollution effect in Helmholtz problems by local subspace correction*, Math. Comput., 86 (2017), pp. 1005–1036.

[45] A. S. Pikovsky and D. L. Shepelyansky, *Destruction of Anderson localization by a weak nonlinearity*, Phys. Rev. Lett., 100 (2008), p. 094101.

[46] J. M. Sanz-Serna, *Methods for the numerical solution of the nonlinear Schrödinger equation*, Math. Comput., 43 (1984), pp. 21–27.

[47] C. Schwab and R. A. Todor, *Karhunen-Loéve approximation of random fields by generalized fast multipole methods*, J. Comput. Phys., 217 (2006), pp. 100–122. Uncertainty Quantification in Simulation Science.

[48] D. L. Shepelyansky, *Delocalization of quantum chaos by weak nonlinearity*, Phys. Rev. Lett., 70 (1993), pp. 1787–1790.

[49] M. E. Taylor, *Partial Differential Equations III: Nonlinear Equations*, Applied Mathematical Sciences, Springer New York, 2010.

[50] M. Thalhammer, *High-order exponential operator splitting methods for time-dependent Schrödinger equations*, SIAM J. Numer. Anal., 46 (2008), pp. 2022–2038.

[51] J. Wang, *A new error analysis of Crank-Nicolson Galerkin FEMs for a generalized nonlinear Schrödinger equation*, J. Sci. Comput., 60 (2014), pp. 390–407.

[52] Z. Wu and Z. Zhang, *Convergence analysis of the localized orthogonal decomposition method for the semiclassical Schrödinger equations with multiscale potentials*, J. Sci. Comput., 93 (2022), p. 73.

[53] Z. Wu, Z. Zhang, and X. Zhao, *Error estimate of a quasi-Monte Carlo time-splitting pseudospectral method for nonlinear Schrödinger equation with random potentials*, SIAM/ASA J. Uncertainty Quantif., 12 (2024), pp. 1–29.

[54] X. Zhao, *Numerical integrators for continuous disordered nonlinear Schrödinger equation*, J. Sci. Comput., 89 (2021), p. 40.

[55] G. E. ZOURARIS, *On the convergence of a linear two-step finite element method for the nonlinear Schrödinger equation*, ESAIM: M2AN, 35 (2001), pp. 389–405.